

# Log( $1/x$ ) Gluon Distribution and Structure Functions in the Loop-Loop Correlation Model

H. J. Pirner<sup>1,\*</sup>, A. I. Shoshi<sup>1,†</sup>, and G. Soyez<sup>2,‡</sup>

<sup>1</sup>*Institut für Theoretische Physik, Universität Heidelberg,  
Philosophenweg 19, D-69120 Heidelberg, Germany*

<sup>2</sup>*Inst. de Physique, Bât. B5, Université de Liège,  
Sart-Tilman, B4000 Liège, Belgium*

We consider the interaction of the partonic fluctuation of a scalar “photon” with an external color field to calculate the leading and next-to-leading order gluon distribution of the proton following the work done by Dosch-Hebecker-Metz-Pirner [1]. We relate these gluon distributions to the short and long distance behavior of the cross section of an adjoint dipole scattering off a proton. The leading order result is a constant while the next-to-leading order result shows a  $\ln(1/x)$  enhancement at small  $x$ . To get numerical results for the gluon distributions at the initial scale  $Q_0^2 = 1.8 \text{ GeV}^2$ , we compute the adjoint dipole-proton cross section in the loop-loop correlation model. Quark distributions at the same initial scale are parametrized according to Regge theory. We evolve quark and gluon distributions to higher  $Q^2$  values using the DGLAP equation and compute charm and proton structure functions in the small- $x$  region for different  $Q^2$  values.

Keywords: Gluon Distribution, Quark Distribution, High-Energy Scattering, Non-Perturbative QCD, DGLAP Evolution, Regge Theory, Charm Structure Function, Proton Structure Function.

PACS numbers: 11.80.Fv, 12.38.-t, 12.40.-y, 13.60.-r.

## I. INTRODUCTION

The understanding of deep inelastic scattering (DIS) in the small- $x$  regime remains one of the challenges in quantum chromodynamics (QCD). Perturbative and nonperturbative physics are important for a complete picture of the small- $x$  limit of structure functions. In this work, we combine perturbative and nonperturbative approaches to describe charm and proton structure functions (or quark and gluon distributions) in the small- $x$  region.

The basic idea is the description of high-energy scattering in QCD by studying the eikonalized interaction of energetic partons with external color fields. In ref. [1], this semiclassical method has been compared with the parton model to extract the leading order (LO) and next-to-leading order (NLO) gluon distribution. The main idea is simple and goes back to Mueller [2]. One calculates the gluon production cross section for a scalar “photon”, which directly couples to the gluon field, in an external color field. The calculation of one-gluon production leads to the LO gluon distribution and the one of two-gluon production to the NLO gluon distribution. The LO result turns out to be a constant,  $xg^{(0)}(x, Q^2) \propto \text{const.}$ , characterising the averaged local field strength in the proton. The NLO result shows a logarithmic increase at small  $x$ ,  $xg^{(1)}(x, Q^2) \propto \ln(1/x)$ , and is sensitive to the large distance structure of the proton.

In order to make numerical estimates for the gluon distributions, we relate the LO and NLO gluon distributions to the scattering of a dipole in the adjoint representation of  $SU(3)$  on a proton. Then, we use the loop-loop correlation model (LLCM) [3] to compute this adjoint dipole - proton cross section at the center of mass (c.m.) energy of  $\sqrt{s_0} \approx 20 \text{ GeV}$ . The two gluons emerging from the scalar “photon” represent the adjoint dipole and a fundamental quark-diquark dipole models the proton in the LLCM. The correlation between the two dipoles given by Wegner-Wilson loops is evaluated in the Gaussian approximation of gluon field strengths. The perturbative interactions are obtained from perturbation theory and the nonperturbative gluon field strength correlator is parametrized in line with simulations in the lattice QCD. The calculation of scattering cross sections in the loop-loop correlation model has been quite successful at low energies  $\sqrt{s_0} \approx 20 \text{ GeV}$  [3, 4, 5, 6, 7].

For small virtuality  $Q^2$ , the perturbative wave function of the two gluons emerging from the scalar “photon” is unrealistically extended at the endpoints of the longitudinal momentum fraction  $\alpha = 0, 1$ . This problem is similar to the quark-antiquark wave function of the transverse photon. The phenomenological solution we propose is to give the gluon a constituent mass  $m_G$  of the order of the rho mass. This mass modifies the wave function at small transverse gluon momenta  $k_\perp$  ensuring “confinement” for the two gluons, but does not affect the perturbative part of the two-gluon wave function at high  $k_\perp$ .

We calculate the  $x$ -dependence of the gluon distribution at a scale  $Q_0^2 = 1.8 \text{ GeV}^2$  which corresponds to the upper limit where the nonperturbative input is still credible. The quark distributions at the same scale are

\*E-mail address: pir@tphys.uni-heidelberg.de

†E-mail address: shoshi@tphys.uni-heidelberg.de

‡E-mail address: g.soyez@ulg.ac.be

parametrized in line with Regge theory [8]. We evolve both distributions to higher values of  $Q^2$  using DGLAP equations [9]. With quark and gluon distributions, we compute charm and proton structure functions at small  $x$  for different  $Q^2$  values in good agreement with experimental data.

The outline of the paper is as follows: In section II we review the formulas for the calculation of the LO and NLO gluon distribution following [1], introduce a gluon mass into the formalism and rewrite the final expressions for gluon distributions in terms of adjoint dipole-proton cross sections. We compute the adjoint dipole-proton cross section in the loop-loop correlation model in section III. In section IV we determine the  $x$  dependence of the quark distributions at the initial scale  $Q_0^2$  according to Regge theory. The initial gluon and quark distributions are evolved to higher virtualities  $Q^2$  using the DGLAP equation. In section V we present the results for the charm and proton structure function versus Bjorken- $x$  at different  $Q^2$  values. Finally, in section VI, we summarize our results.

## II. THE SEMI-CLASSICAL GLUON DISTRIBUTION

In this section we review the formulas for the computation of the LO and NLO gluon distribution [38] in the semiclassical approach and parton model following the work by Dosch, Hebecker, Metz and Pirner [1]. In addition, we introduce a gluon mass in the formalism to take into account the spatial localization of the two gluons due to confinement. We derive the modifications due to massive gluons and rewrite the final results for the gluon distributions in terms of adjoint dipole-proton cross sections.

### A. Gluon distribution at leading order

In order to extract the gluon distribution, we consider a scalar field  $\chi$  (or scalar “photon”) coupled directly to the gluon field through the interaction lagrangian

$$\mathcal{L}_I = -\frac{\lambda}{2}\chi\text{tr}(\mathbf{F}_{\mu\nu}\mathbf{F}^{\mu\nu}) ,$$

with  $\mathbf{F}_{\mu\nu} = F_{\mu\nu}^a t^a$ , the gluon field strength  $F_{\mu\nu}^a = [\partial_\mu A_\nu^a - \partial_\nu A_\mu^a - gf^{abc}A_\mu^b A_\nu^c]$ , the gluon field  $A^a$  and the  $SU(N_c)$  group generators in the adjoint representation  $t^a$ . In the high-energy limit, the scattering of a  $\chi$ -particle off an external color field  $A^a$  as shown in Fig. 1(a), has the following amplitude

$$\mathcal{T}^a(b_\perp) = \frac{i\lambda q_0}{2C_A} \int dx_+ \text{tr} [t^a(\epsilon_\perp^* \partial_\perp) A^A(x_+, b_\perp)] .$$

Here  $b_\perp$  denotes the impact parameter in transverse space,  $q$  the four momentum vector of the  $\chi$ -particle,

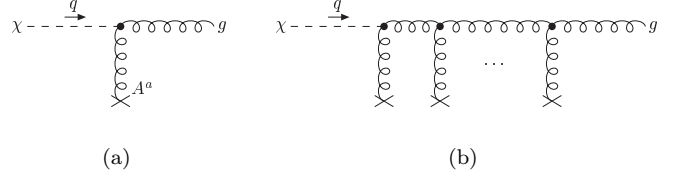


FIG. 1: The process  $\chi \rightarrow g$  in an external color field: (a) one gluon exchange, (b) resummed gluon exchange.

$x_+ = x_0 + x_3$  the light-cone variable,  $\partial_\perp \equiv \partial/\partial b_\perp$ ,  $A^A = A^b t^b$  the external color field,  $C_A = N_c$  the Casimir operator in the adjoint representation,  $N_c$  the number of colors and  $\epsilon_\perp$  the polarisation vector of the outgoing gluon.

Resumming the gluon exchange to all orders as shown in Fig. 1(b), the gluon initially created at the vertex  $\chi gg$  acquires a non-abelian eikonal factor on the way through the external color field

$$U_{(\infty, x_+)}^A(b_\perp) = P \exp \left[ -\frac{ig}{2} \int_{x_+}^{\infty} dx_+ A^A(x_+, b_\perp) \right] .$$

The path ordering along the way  $x_+$  is denoted by  $P$ . With

$$W_{b_\perp}^A(r_A) = U^A(b_\perp - r_A/2) U^{A\dagger}(b_\perp + r_A/2) - \mathbb{1} , \quad (1)$$

where the eikonal factors  $U^A(b_\perp - r_A/2) \equiv U_{\infty, -\infty}^A(b_\perp - r_A/2)$  and  $U^{A\dagger}(b_\perp + r_A/2)$  come from the scattering of two gluons (moving in opposite directions) with transverse distance  $r_A$  off the proton, the semiclassical (sc) cross-section for gluon production at leading order becomes (cf. ref. [1])

$$\sigma_{\text{sc}}^{(0)} = \frac{\lambda^2}{4g^2 C_A} \int d^2 b_\perp \left| [\partial_{r_A} W_{b_\perp}^A(r_A)]_{r_A=0} \right|^2 . \quad (2)$$

In the following an average over the external color fields underlying the quantity  $W_{b_\perp}^A$  is implicitly understood.

On the other hand, the leading-order parton model (pm) cross section for the partonic process  $\chi g \rightarrow g$  shown in Fig. 2 with the proton described by the gluon distribution is given by

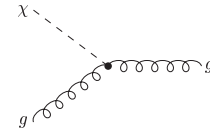


FIG. 2: The process  $\chi g \rightarrow g$  in the parton model.

bution is given by

$$\sigma_{\text{pm}}^{(0)} = \frac{\pi\lambda}{4} x g^{(0)}(x, Q^2) . \quad (3)$$

Identifying the semiclassical cross-section (2) with the partonic one (3), one finds the leading-order gluon distribution

$$xg^{(0)}(x, Q^2) = \frac{1}{2\pi^2\alpha_s} \frac{1}{2C_A} \int d^2b_\perp \left| [\partial_{r_A} W_{b_\perp}^A(r_A)]_{r_A=0} \right|^2. \quad (4)$$

Using the expression for the adjoint dipole (d) - proton (p) cross section in the semiclassical approach [1, 10]

$$\sigma_{sc}^{dp}(r_A) = -\frac{2}{3} \int d^2b_\perp \text{tr} W_{b_\perp}^A(r_A) \quad (5)$$

and the identity

$$\int d^2b_\perp \left| [\partial_{r_A} W_{b_\perp}^A(r_A)]_{r_A=0} \right|^2 = - \left[ \partial_{r_A}^2 \int d^2b_\perp \text{tr} W_{b_\perp}^A(r_A) \right]_{r_A=0} \quad (6)$$

one can rewrite eq. (4) in the useful form

$$xg^{(0)}(x, Q^2) = \frac{3}{4\pi^2\alpha_s} \frac{1}{2C_A} [\partial_{r_A}^2 \sigma_{sc}^{dp}(r_A)]_{r_A=0}. \quad (7)$$

This equation shows that the LO gluon distribution depends on the small distance behavior of the adjoint dipole-proton cross section. To get numerical results for the gluon distribution, we use in the next section a model to compute the adjoint dipole-proton cross section.

## B. Gluon distribution at next-to-leading order

For the semiclassical calculation of the gluon distribution at next-to-leading order, the three diagrams shown in Fig. 3 are relevant in the high energy limit. Resumming the interaction with the external field to all orders, i. e., repeating the step leading from Fig. 1(a) to Fig. 1(b), we obtain the result shown in Fig. 4. In the first diagram the incoming  $\chi$ -particle splits into two gluons before interacting with the target. The subsequent scattering of the two gluons off the external color field is treated in the eikonal approximation. In the second diagram the two fast gluons are created through a  $\chi g g g$  vertex in the space-time region of the external color field.

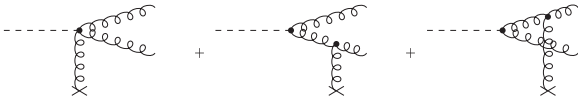


FIG. 3: Diagrams contributing to the  $\chi \rightarrow gg$  amplitude in the high-energy limit.

One can show [1] that the amplitudes in Fig. 4 produce the following NLO contribution to the cross-section

$$\sigma_{sc}^{(1)}(x, Q^2) = \frac{\lambda^2}{32(2\pi)^6} \int \frac{d\alpha}{\alpha(1-\alpha)} \int dk_\perp'^2 \int d^2b_\perp \left| \int d^2k_\perp \frac{N^2 \delta_{ij} + 2k_i k_j}{N^2 + k_\perp^2 + m_G^2} \tilde{W}_{b_\perp}^A(k'_\perp - k_\perp) \right|^2, \quad (8)$$

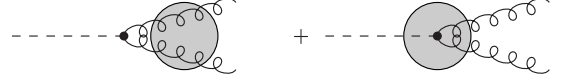


FIG. 4: Relevant contributions in the NLO semiclassical calculation.

where  $\alpha$  and  $1-\alpha$  are the longitudinal momentum carried by the two gluons,  $k_\perp$  and  $k'_\perp$  are the transverse momenta of one of the two gluons before and after the interaction with the external field,  $N^2 = \alpha(1-\alpha)Q^2$  and  $\tilde{W}_{b_\perp}^A(k_\perp)$  is the Fourier transform of  $W_{b_\perp}^A(r_A)$  given in eq. (1).

In equation (8) we have introduced a gluon mass  $m_G$  into the gluon propagator. This mass mimics the confinement of the two gluons emerging from the  $\chi$ -particle and modifies their perturbative wave function in the non-perturbative, small  $k_\perp$  region for small virtualities  $Q^2$  or momentum fractions  $\alpha = 0, 1$ . Phenomenologically, the gluon mass has a similar effect as a constituent quark mass in the perturbative quark-antiquark wave function of the transverse photon [11]. We use for the gluon mass  $m_G = 770$  MeV, i.e., approximately half of the glueball mass.

To compute the NLO contribution to the gluon distribution in the parton model, we have to calculate the diagrams shown in Fig. 5. With  $z = Q^2/(Q^2 + s) = x/y$ ,

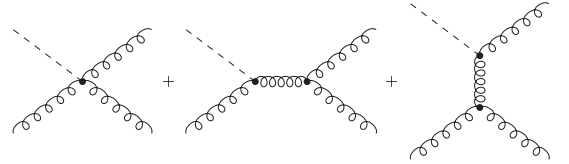


FIG. 5: Diagrams contributing to the parton model at NLO.

where  $y$  is the fraction of the target momentum carried by the struck gluon, the parton model cross-section at NLO reads

$$\sigma_{pm}(x, Q^2) = \int_x^1 \frac{dz}{z} \left[ \sigma_d^{(0)} \delta(1-x) + \hat{\sigma}^{(1)}(x, Q^2) \right] y g_b(y), \quad (9)$$

with  $\sigma_d^{(0)} = (\pi\lambda_d^2)/4$  and the  $d = (4 + \epsilon)$  dimensional coupling  $\lambda_d = \lambda\mu^{-\epsilon/2}$ . Since we are interested in the high energy limit, we extract only the leading term in  $\ln(1/x)$  from the expression in (9). We regularize the bare gluon distribution  $g_b(x)$  in the  $\overline{\text{MS}}$  scheme

$$g_b(x) = g(x, \mu^2) - \frac{\alpha_s}{2\pi} \int_x^1 \frac{dz}{z} P_{gg}(z) \left[ \frac{2}{\epsilon} + \gamma_E - \ln(4\pi) \right] g(y, \mu^2),$$

with  $P_{gg}$  denoting the gluon-gluon splitting function.

The parton model cross-section at NLO finally becomes

$$\sigma_{\text{pm}} = \sigma_{d=4}^{(0)} x \int_x^1 \frac{dz}{z} g(y, \mu^2) \left\{ \delta(1-z) + \frac{\alpha_s}{2\pi} \left[ P_{gg}(z) \ln \left( \frac{Q^2}{\mu^2} \right) + C_g^{\overline{\text{MS}}}(z) \right] \right\}, \quad (10)$$

where

$$C_g^{\overline{\text{MS}}}(z) = P_{gg}(z) \ln \left( \frac{1-z}{z} \right) - \frac{11C_A}{6z(1-z)}.$$

Expanding the full gluon distribution up to the order  $\ln(1/x)$

$$xg(x, \mu^2) = xg^{(0)}(x, \mu^2) + xg^{(1)}(x, \mu^2),$$

and identifying (8) with (10), we obtain

$$\begin{aligned} xg^{(1)}(x, \mu^2) &= \frac{1}{4(2\pi)^7} \int \frac{d\alpha}{\alpha(1-\alpha)} \int dk_{\perp}'^2 \int d^2b_{\perp} \\ &\times \left| \int d^2k_{\perp} \frac{N^2 \delta_{ij} + 2k_i k_j}{N^2 + k_{\perp}^2 + m_G^2} \tilde{W}_{b_{\perp}}^A(k'_{\perp} - k_{\perp}) \right|^2 \\ &- \frac{\alpha_s}{2\pi} \int_x^1 dz \left[ P_{gg}(z) \ln \left( \frac{Q^2}{\mu^2} \right) + C_g^{\overline{\text{MS}}}(z) \right] yg^{(0)}(y, \mu^2), \end{aligned} \quad (11)$$

where  $g^{(0)}(x, \mu^2)$  is given by (4). When evaluating equation (11), we keep only  $\ln(1/x)$  terms, i.e., we use

$$\begin{aligned} P_{gg}(z) &\approx \frac{2C_A}{z}, \\ C_g^{\overline{\text{MS}}}(z) &\approx \frac{2C_A}{z} \left[ \ln \left( \frac{1}{z} \right) - \frac{11}{12} \right]. \end{aligned}$$

Using the variable  $z = Q^2/(Q^2 + M^2)$ , with  $M^2 = k_{\perp}'^2/(\alpha(1-\alpha))$ , and introducing a scale  $\kappa^2$  such that  $\Lambda_{QCD}^2 \ll \kappa^2 \ll Q^2$ , the first contribution in (11) can be split into a hard and a soft component [1, 10]

$$\begin{aligned} &\frac{1}{4(2\pi)^7} \int \frac{d\alpha}{\alpha(1-\alpha)} \int dk_{\perp}'^2 \int d^2b_{\perp} \\ &\times \left| \int d^2k_{\perp} \frac{N^2 \delta_{ij} + 2k_i k_j}{N^2 + k_{\perp}^2 + m_G^2} \tilde{W}_{b_{\perp}}^A(k'_{\perp} - k_{\perp}) \right|^2 \\ &= \frac{1}{4\pi^3} \int_x^1 \frac{dz}{z} \ln \left( \frac{Q^2}{z\kappa^2} \right) \int d^2b_{\perp} \left| [\partial_{r_A} W_{b_{\perp}}^A(r_A)]_{r_A=0} \right|^2 \\ &+ \frac{2}{\pi} \int_x^1 \frac{dz}{z} \int_0^{\kappa^2} dk_{\perp}'^2 f(k_{\perp}'^2), \end{aligned} \quad (12)$$

where

$$\begin{aligned} f(k_{\perp}'^2) &= \int \frac{d^2r_A}{(2\pi)^2 r_A^2} \int \frac{d^2r_A'}{(2\pi)^2 r_A'^2} \int d^2b_{\perp} \\ &\text{tr} \left[ W_{b_{\perp}}^A(r_A) W_{b_{\perp}}^{A\dagger}(r_A') \right] e^{ik_{\perp}'(r_A - r_A')} H(r_A, r_A'), \\ H &= \frac{(r_A \cdot r_A')^2}{r_A^2 r_A'^2} [\hat{a}^2 K_0(\hat{a})] [\hat{b}^2 K_0(\hat{b})] \\ &+ \frac{1}{2} \left[ \frac{2(r_A \cdot r_A')^2}{r_A^2 r_A'^2} - 1 \right] \left\{ [\hat{a} K_1(\hat{a})] [\hat{b} K_1(\hat{b})] \right. \\ &\quad \left. + [\hat{a} K_1(\hat{a})] [\hat{b}^2 K_0(\hat{b})] \right. \\ &\quad \left. + [\hat{a}^2 K_0(\hat{a})] [\hat{b} K_1(\hat{b})] \right\}, \end{aligned}$$

with  $\hat{a} = m_G r_A$  and  $\hat{b} = m_G r_A'$ . Note that the gluon mass does not influence the hard part which is calculated at leading twist. The lower bound of the  $z$  integration,  $x \leq z$ , is a kinematical limit ensuring that the invariant mass of the two produced gluons cannot be larger than the total center-of-mass energy available [1, 10].

Inserting (12) in (11), the  $\ln^2(1/x)$  terms from the semiclassical and the parton calculations cancel, so that

$$\begin{aligned} xg^{(1)}(x, \mu^2) &= \ln \left( \frac{1}{x} \right) \left\{ \frac{2}{\pi} \int_0^{\kappa^2} dk_{\perp}'^2 f(k_{\perp}'^2) \right. \\ &\quad \left. + \frac{\alpha_s}{\pi} C_A \left[ \ln \left( \frac{\kappa^2}{\mu^2} \right) + \frac{11}{12} \right] xg^{(0)} \right\}. \end{aligned}$$

For  $\kappa^2 = \mu^2 \exp(11/12)$ , the second term also drops out and one obtains

$$xg^{(1)}(x, \mu^2) = \frac{2}{\pi} \ln \left( \frac{1}{x} \right) \int_0^{e^{11/12} \mu^2} dk_{\perp}'^2 f(k_{\perp}'^2). \quad (13)$$

After the integration over  $k_{\perp}'^2$  and  $r_A'$ , the NLO correction to the gluon distribution becomes [1, 10]

$$\begin{aligned} xg^{(1)}(x, \mu^2) &= \frac{1}{2\pi^3} \ln \left( \frac{1}{x} \right) \int_{r_0^2(\mu^2)}^{\infty} \frac{dr_A^2}{r_A^2} m_G^2 F(m_G r_A) \\ &\times \int d^2b_{\perp} \text{tr} \left[ W_{b_{\perp}}^A(r_A) W_{b_{\perp}}^{A\dagger}(r_A) \right] \end{aligned} \quad (14)$$

where

$$\begin{aligned} r_0^2(\mu^2) &= \frac{4e^{\frac{1}{12} - 2\gamma_E}}{\mu^2}, \\ F(z) &= K_1^2(z) + zK_0(z)K_1(z) + \frac{z^2}{2}K_0^2(z) \\ &= \frac{z^2}{2}K_2^2(z) - zK_1(z)K_2(z) + K_1^2(z). \end{aligned}$$

In the large- $N_c$  limit [12], one obtains the relation

$$\int d^2b_{\perp} \text{tr} \left[ W_{b_{\perp}}^A(r_A) W_{b_{\perp}}^{A\dagger}(r_A) \right] = -2 \int d^2b_{\perp} \text{tr} W_{b_{\perp}}^A(r_A)$$

which allows us to rewrite the NLO correction in terms of the dipole-proton cross section (5)

$$xg^{(1)}(x, \mu^2) = \ln\left(\frac{1}{x}\right) \frac{3m_G^2}{2\pi^2} \int_{r_0^2(\mu^2)}^{\infty} \frac{dr_A^2}{r_A^2} F(m_G r_A) \sigma_{sc}^{dp}(r_A). \quad (15)$$

The NLO gluon distribution depends on the large distance behavior of the adjoint dipole-proton cross section. For small  $r_A$  the function  $F(m_G r_A)$  reduces to  $1/(m_G r_A)^2$ , and eq. (15) shows qualitative agreement with eqs. (49)-(50) of Mueller [2]. To obtain numerical results for the LO and NLO gluon distribution, we calculate the dipole-proton cross section at some low c.m. energy  $\sqrt{s_0}$  within the loop-loop correlation model in the following section.

### III. DIPOLE-PROTON CROSS SECTION FROM THE LOOP-LOOP CORRELATION MODEL

In this section we use the loop-loop correlation model (LLCM) [3] to compute the cross section of an adjoint dipole scattering off a proton,  $\sigma_{sc}^{dp}(r_A, s_0)$ , at the c.m. energy  $\sqrt{s_0} = 20$  GeV. Then, we insert the resulting dipole-proton cross section in eqs. (7) and (15) to calculate the LO and NLO gluon distributions.

The loop-loop correlation model is based on the functional integral approach to high-energy scattering in the eikonal approximation [4, 5, 6, 7]. Its central elements are gauge-invariant Wegner-Wilson loops. With a phenomenological energy dependence, we have shown that the LLCM allows a unified description of high-energy hadron-hadron, photon-hadron, and photon-photon reactions [3, 13, 14] and of static properties of hadrons [15, 16] in agreement with experimental and lattice data. In this work, we do not need a phenomenological parametrization for the energy dependence since this is generated by the formalism outlined in the sections before.

In the framework of LLCM the adjoint dipole - proton cross section reads [3, 13]

$$\sigma_{LLCM}^{dp}(r_A, s_0) = 2 \int d^2 b_{\perp} \int \frac{d\phi_A}{2\pi} \int d^2 r_{\mathcal{F}} dz_q |\psi_p(z_q, \vec{r}_{\mathcal{F}})|^2 \times \left(1 - S^{\mathcal{A}\mathcal{F}}(s_0, \vec{b}_{\perp}, \vec{r}_A, z_q, \vec{r}_{\mathcal{F}})\right). \quad (16)$$

Here the correlation of two light-like Wegner-Wilson loops

$$S^{\mathcal{A}\mathcal{F}}(s_0, \vec{b}_{\perp}, \vec{r}_A, z_q, \vec{r}_{\mathcal{F}}) = \frac{\langle \mathcal{W}^{\mathcal{A}}[C_g] \mathcal{W}^{\mathcal{F}}[C_q] \rangle_G}{\langle \mathcal{W}^{\mathcal{A}}[C_g] \rangle_G \langle \mathcal{W}^{\mathcal{F}}[C_q] \rangle_G}, \quad (17)$$

describes the elastic scattering of a dipole in the fundamental ( $\mathcal{F}$ ) with a dipole in the adjoint ( $\mathcal{A}$ ) representation of  $SU(N_c)$ . In the present case where a  $\chi$ -particle scatters off a proton, the adjoint color-dipole is given by

the two gluons in the color-singlet state emerging from the  $\chi$ -particle and the fundamental color-dipole is given in a simplified picture by a quark and diquark in the proton [39]. Each color-dipole is represented by a light-like Wegner-Wilson loop [18]

$$\mathcal{W}^r[C] = \tilde{\text{Tr}}_r \mathcal{P} \exp \left[ -ig \oint_C dz^\mu A_\mu^a(z) t_r^a \right],$$

where the subscript  $r$  indicates the representation of  $SU(N_c)$ ,  $\tilde{\text{Tr}}_r = \text{Tr}_r(\dots)/\text{Tr} \mathbb{1}_r$  is the normalized trace in the corresponding color-space with unit element  $\mathbb{1}_r$ , and  $A_\mu(z) = A_\mu^a(z) t_r^a$  represents the gluon field with the  $SU(N_c)$  group generators in the corresponding representation,  $t_r^a$ , that demand the path ordering indicated by  $\mathcal{P}$  on the closed path  $C$  in space-time. Physically, the Wegner-Wilson loop represents the phase factor acquired by a color-charge in the  $SU(N_c)$  representation  $r$  along the light-like trajectory  $C$  in the gluon background field.

The color-dipoles have transverse size and orientation  $\vec{r}_{\mathcal{A},\mathcal{F}}$ . The longitudinal momentum fraction of the dipole carried by the quark (gluon) is  $z_q$  ( $z_g$ ). The impact parameter between the dipoles is [19]

$$\vec{b}_{\perp} = \vec{r}_g + (1 - z_g)\vec{r}_A - \vec{r}_q - (1 - z_q)\vec{r}_{\mathcal{F}} = \vec{r}_{\mathcal{A}cm} - \vec{r}_{\mathcal{F}cm},$$

where  $\vec{r}_q$ ,  $\vec{r}_{qq}$ ,  $\vec{r}_g$ , and  $\vec{r}_{\bar{g}}$  are the transverse positions of the quark, diquark, gluon and the gluon moving in the opposite direction, respectively. With  $\vec{r}_{\mathcal{F}} = \vec{r}_{qq} - \vec{r}_q$  and  $\vec{r}_{\mathcal{A}} = \vec{r}_{\bar{g}} - \vec{r}_g$ , the center of light-cone momenta of the two dipoles are given by  $\vec{r}_{\mathcal{A}cm} = z_g \vec{r}_g + (1 - z_g) \vec{r}_{\bar{g}}$  and  $\vec{r}_{\mathcal{F}cm} = z_q \vec{r}_q + (1 - z_q) \vec{r}_{qq}$ . Figure 6 illustrates the (a) space-time and (b) transverse arrangement of the dipoles.

The QCD vacuum expectation value  $\langle \dots \rangle_G$  in the loop-loop correlation function (17) represents functional integrals [5] over gluon field configurations: the functional integration over the fermion fields has already been carried out as indicated by the subscript  $G$ . The model we use for the QCD vacuum describes only gluon dynamics and, thus, implies the quenched approximation that does not allow string breaking through dynamical quark-antiquark production.

The  $\vec{r}_{\mathcal{F}}$  and  $z_q$  distribution of the fundamental color-dipole in the proton is given by the proton wave function  $\psi_p$ . We use for the proton wave function the phenomenological Gaussian Wirbel-Stech-Bauer ansatz [20]

$$\psi_p(z_q, \vec{r}_{\mathcal{F}}) = \sqrt{\frac{z_q(1 - z_q)}{2\pi S_p^2 N_p}} e^{-(z_q - \frac{1}{2})^2 / (4\Delta z_p^2)} e^{-|\vec{r}_{\mathcal{F}}|^2 / (4S_p^2)}.$$

The constant  $N_p$  is fixed by the normalization of the wave function to unity, the extension parameter  $S_p$  is approximately given by the electromagnetic radius of the proton and the width  $\Delta z_p = w/(\sqrt{2}m_p)$  [20] is determined by the proton mass  $m_p$  and the value  $w = 0.35 - 0.5$  GeV extracted from experimental data. We adopt the values  $\Delta z_p = 0.3$  and  $S_p = 0.86$  fm which have allowed a good description of many high-energy scattering data in our previous work [3].

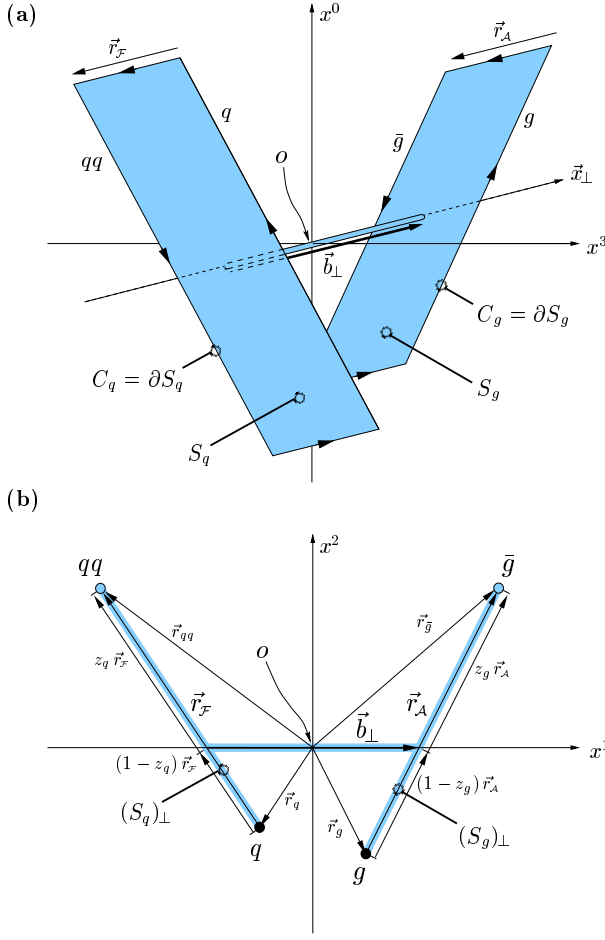


FIG. 6: High-energy scattering of a fundamental dipole with an adjoint dipole in the eikonal approximation represented by Wegner-Wilson loops: (a) space-time and (b) transverse arrangement of the Wegner-Wilson loops. The shaded areas represent the strings extending from the quark (gluon) to the diquark (antigluon) path in each color dipole. The thin tube allows to compare the field strengths in surface  $S_q$  with the field strengths in surface  $S_g$ . The impact parameter  $\vec{b}_\perp$  connects the centers of light-cone momenta of the dipoles.

The computation of the loop-loop correlation for one dipole in the fundamental and the other one in the adjoint representation of  $SU(N_C)$  can be found in detail in [13, 15, 16]. The main steps of this computation are the transformation of the line integrals in the Wegner-Wilson loops into surface integrals with the non-Abelian Stokes theorem, a matrix cumulant expansion, and the Gaussian approximation of the functional integrals in the gluon

field strengths. These steps lead to the following result

$$\frac{\langle \mathcal{W}^A[C_g] \mathcal{W}^F[C_q] \rangle_G}{\langle \mathcal{W}^A[C_g] \rangle_G \langle \mathcal{W}^F[C_q] \rangle_G} = \frac{1}{N_c^2 - 1} \exp\left[i \frac{N_c}{2} \chi\right] + \frac{N_c + 2}{2(N_c + 1)} \exp\left[-i \frac{1}{2} \chi\right] + \frac{N_c - 2}{2(N_c - 1)} \exp\left[i \frac{1}{2} \chi\right] \quad (18)$$

which, for  $N_c = 3$ , corresponds to the well-known  $SU(3)$  decomposition

$$3 \otimes 8 = 3 \oplus 15 \oplus 6.$$

The function  $\chi := \chi^P + \chi_{nc}^{NP} + \chi_c^{NP}$  has the following form [3]:

$$\begin{aligned} \chi^P = & \left[ g^2 (\vec{r}_g - \vec{r}_q) iD_P'^{(2)} (\vec{r}_g - \vec{r}_q) \right. \\ & + g^2 (\vec{r}_{\bar{g}} - \vec{r}_{qq}) iD_P'^{(2)} (\vec{r}_{\bar{g}} - \vec{r}_{qq}) \\ & - g^2 (\vec{r}_g - \vec{r}_{qq}) iD_P'^{(2)} (\vec{r}_g - \vec{r}_{qq}) \\ & \left. - g^2 (\vec{r}_{\bar{g}} - \vec{r}_q) iD_P'^{(2)} (\vec{r}_{\bar{g}} - \vec{r}_q) \right], \end{aligned} \quad (19)$$

$$\begin{aligned} \chi_{nc}^{NP} = & \frac{\pi^2 G_2 (1 - \kappa)}{3(N_c^2 - 1)} \left[ iD_1'^{(2)} (\vec{r}_g - \vec{r}_q) + iD_1'^{(2)} (\vec{r}_{\bar{g}} - \vec{r}_{qq}) \right. \\ & \left. - iD_1'^{(2)} (\vec{r}_g - \vec{r}_{qq}) - iD_1'^{(2)} (\vec{r}_{\bar{g}} - \vec{r}_q) \right], \end{aligned} \quad (20)$$

$$\begin{aligned} \chi_c^{NP} = & \frac{\pi^2 G_2 \kappa}{3(N_c^2 - 1)} (\vec{r}_A \cdot \vec{r}_F) \\ & \times \int_0^1 dv_A \int_0^1 dv_F iD^{(2)} (\vec{r}_g + v_A \vec{r}_A - \vec{r}_q - v_F \vec{r}_F), \end{aligned} \quad (21)$$

with the perturbative ( $iD_P'^{(2)}$ ) and nonperturbative ( $iD_1'^{(2)}$  and  $iD^{(2)}(\vec{z}_\perp)$ ) correlation functions in transverse space

$$iD_P'^{(2)}(\vec{z}_\perp) = \frac{1}{2\pi} K_0(m_G |\vec{z}_\perp|), \quad (22)$$

$$iD_1'^{(2)}(\vec{z}_\perp) = \pi a^4 [3 + 3(|\vec{z}_\perp|/a) + (|\vec{z}_\perp|/a)^2] \exp(-|\vec{z}_\perp|/a), \quad (23)$$

$$iD^{(2)}(\vec{z}_\perp) = 2\pi a^2 [1 + (|\vec{z}_\perp|/a)] \exp(-|\vec{z}_\perp|/a). \quad (24)$$

We have introduced in the perturbative component  $\chi^P$  the same effective gluon mass  $m_G = 0.77 \text{ GeV}$  as before to limit the range of the perturbative interaction in the infrared region and a parameter  $M^2 = 1.04 \text{ GeV}^2$  which freezes the running coupling in the quenched approximation at the value  $g^2(\vec{z}_\perp)/(4\pi) = \alpha_s(k_\perp^2 = 0) = 0.4$  [3],

$$g^2(\vec{z}_\perp) = \frac{48\pi^2}{(33 - 2N_f) \ln \left[ (|\vec{z}_\perp|^{-2} + M^2)/\Lambda_{QCD}^2 \right]}. \quad (25)$$

In Eq. (22)  $K_0$  denotes the  $0^{th}$  modified Bessel function (McDonald function). The non-perturbative correlators (20) and (21) involve the gluon condensate  $G_2 := \langle \frac{g^2}{4\pi^2} F_{\mu\nu}^a(0) F_{\mu\nu}^a(0) \rangle = 0.074 \text{ GeV}^4$ , the parameter  $\kappa = 0.74$  that determines the relative weight of the two different components and the correlation length  $a = 0.302 \text{ fm}$  that enters through the non-perturbative correlation functions  $D$  and  $D_1$ .

The component  $\chi^P$  describes the perturbative interaction of the quark and diquark of the dipole in the proton with the two gluons of the adjoint dipole emerging from the  $\chi$ -particle as evident from (19) and Fig. 6b. The component  $\chi_{nc}^{NP}$  has the same structure as  $\chi^P$  and gives the non-perturbative interaction between the quarks and gluons of the two dipoles. The component  $\chi_c^{NP}$  shows a different structure: the integrations over  $v_A$  and  $v_F$  sum non-perturbative interactions between the strings (flux tubes) confining the quark and diquark or the two gluons in the dipoles as visualized in Fig. 6b. As shown in [15, 21, 22], the  $\chi_c^{NP}$  component leads to color-confinement due to a flux tube formation between a static quark-antiquark pair. Manifestations of confinement in high-energy scattering have been analysed in [14].

Since the squared proton wave function  $|\psi_p(z_q, \vec{r}_F)|^2$  is invariant and the  $\chi$ -function changes sign under the replacement  $(\vec{r}_F \rightarrow -\vec{r}_F, z_q \rightarrow 1 - z_q)$

$$\chi(\vec{b}_\perp, z_g, \vec{r}_A, 1 - z_q, -\vec{r}_F) = -\chi(\vec{b}_\perp, z_g, \vec{r}_A, z_q, \vec{r}_F) ,$$

only the real part of the exponentials in eq. (18) survives in the integration over  $\vec{r}_F$  and  $z_q$  so that one obtains

$$\begin{aligned} \frac{\langle \mathcal{W}^A[C_g] \mathcal{W}^F[C_q] \rangle_G}{\langle \mathcal{W}^A[C_g] \rangle_G \langle \mathcal{W}^F[C_q] \rangle_G} &= \frac{1}{N_c^2 - 1} \cos \left[ \frac{N_c}{2} \chi \right] \\ &+ \frac{N_c + 2}{2(N_c + 1)} \cos \left[ \frac{1}{2} \chi \right] \\ &+ \frac{N_c - 2}{2(N_c - 1)} \cos \left[ \frac{1}{2} \chi \right] . \end{aligned} \quad (26)$$

The above expression describes multiple gluonic interactions between two dipoles since  $(\chi^P)^2$  represents the perturbatively well-known two-gluon exchange and  $(\chi^{NP})^2$  the non-perturbative two-point interaction in the dipole-dipole scattering [14]. The higher order terms in the expansion of the cosine functions ensure the  $S$ -matrix unitarity condition which becomes important at very high c.m. energies [3, 13, 23].

The adjoint dipole-proton cross section obtained with the above ingredients at the c.m. energy  $\sqrt{s_0} \approx 20 \text{ GeV}$  shows color-transparency for small dipole sizes,

$$\sigma_{LLCM}^{dp}(s_0, r_A) \approx 9.6 r_A^2 \quad (27)$$

and linear confining behavior at large dipole sizes,

$$\sigma_{LLCM}^{dp}(s_0, r_A) \propto |\vec{r}_A| . \quad (28)$$

Inserting eqs. (27) and (25) into (7), one obtains for the LO gluon distribution (7) at virtuality  $Q_0^2 = 1.8 \text{ GeV}^2$

$$xg^{(0)}(x, Q_0^2) = \frac{3}{4\pi^2 \alpha_s(Q_0^2)} \frac{1}{2C_A} 2 \cdot 9.6 = 0.81 . \quad (29)$$

With our result for  $\sigma_{LLCM}^{dp}(s_0, r_A)$ , the NLO gluon distribution (15) at the same virtuality reads

$$xg^{(1)}(x, Q_0^2) = 0.89 \ln \left( \frac{1}{x} \right) . \quad (30)$$

#### IV. DGLAP EVOLUTION AT HIGH $Q^2$

In this section we give the gluon and quark distributions at an initial scale  $Q_0^2$ . Their evolution to higher values of  $Q^2$  is obtained by the DGLAP equation

$$\begin{aligned} Q^2 \partial_{Q^2} \begin{pmatrix} q_i(x, Q^2) \\ \bar{q}_i(x, Q^2) \\ g(x, Q^2) \end{pmatrix} &= \frac{\alpha_s}{2\pi} \int_x^1 \frac{d\xi}{\xi} \begin{pmatrix} P_{q_i q_j} & 0 & P_{q_i g} \\ 0 & P_{q_i q_j} & P_{q_i g} \\ P_{gq} & P_{gq} & P_{gg} \end{pmatrix} \bigg|_{\frac{x}{\xi}} \begin{pmatrix} q_j(\xi, Q^2) \\ \bar{q}_j(\xi, Q^2) \\ g(\xi, Q^2) \end{pmatrix} , \end{aligned} \quad (31)$$

with the splitting functions  $P_{xy}$  being at leading order  $Q^2$  independent. We use the resulting gluon and quark distributions to compute the charm and proton structure function at different  $x$  and  $Q^2$  values.

The gluon distribution computed in the previous section reads

$$xg(x, Q_0^2) = A [1 + B \ln(1/x)] , \quad (32)$$

with  $A = 0.81$  and  $B = 1.1$  for  $Q_0^2 = 1.8 \text{ GeV}^2$ . Our result, however, is only expected to be valid at low  $x$  values. For large  $x$  values,  $x > x_{\text{GRV}} = 0.15$ , we use the Gluck-Reya-Vogt (GRV) gluon distribution [24]. To match to this gluon distribution at  $x = x_{\text{GRV}}$ , we introduce a scale  $x_0$  in our gluon distribution

$$G(x, Q_0^2) = xg(x, Q_0^2) = A [1 + B \ln(x_0/x)] \quad (33)$$

which takes into account the neglected constant term in the NLO calculation where only the leading  $\ln(1/x)$  terms have been kept. For  $Q_0^2 = 1.8 \text{ GeV}^2$  and  $x_{\text{GRV}} = 0.15$ , we obtain  $x_0 = 0.1454$ .

To calculate the proton structure function  $F_2^p(x, Q^2)$ ,

$$F_2^p(x) = x \sum_{\text{flavours}} e_q^2 [q(x) + \bar{q}(x)] ,$$

with the DGLAP evolution (31), we need quark and gluon distributions, since they are coupled to each other. For the computation of  $F_2^p(x, Q^2)$ , however, only two linear combinations of quark distributions are required

$$\begin{aligned} T &= x(u^+ + c^+ + t^+) - x(d^+ + s^+ + b^+) , \\ \Sigma &= x(u^+ + c^+ + t^+) + x(d^+ + s^+ + b^+) , \end{aligned}$$

since

$$F_2^p = \frac{5\Sigma + 3T}{18},$$

with  $q^+ = q + \bar{q}$  and  $q = u, d, s, c, t, b$ . Performing linear combinations in (31), we can directly check that  $T$ ,  $\Sigma$  and  $G$  evolve according to the following DGLAP equations

$$\begin{aligned} Q^2 \partial_{Q^2} T(x, Q^2) &= \frac{\alpha_s}{2\pi} \int_x^1 \frac{x d\xi}{\xi^2} P_{qq} \left( \frac{x}{\xi} \right) T(\xi, Q^2), \\ Q^2 \partial_{Q^2} \begin{pmatrix} \Sigma(x, Q^2) \\ G(x, Q^2) \end{pmatrix} &= \frac{\alpha_s}{2\pi} \int_x^1 \frac{x d\xi}{\xi^2} \begin{pmatrix} P_{qq} & 2n_f P_{qg} \\ P_{gq} & P_{gg} \end{pmatrix} \bigg|_{\frac{x}{\xi}} \begin{pmatrix} \Sigma(\xi, Q^2) \\ G(\xi, Q^2) \end{pmatrix}, \end{aligned}$$

which means that  $T$  evolves alone, while  $\Sigma$  is coupled with  $G$ .

We determine the  $x$ -dependence of the  $T$  and  $\Sigma$  distribution at the scale  $Q_0^2$  following the ideas from [25]. First, the  $T$ ,  $\Sigma$  and  $G$  distributions are required to have a common singularity structure in the complex  $j$ -plane according to Regge theory. Since the initial gluon distribution (33) has a double pole in  $j = 1$ , consequently, also the  $T$  and  $\Sigma$  distribution are required to have a double-pole pomeron term. Secondly, we add a reggeon contribution (coming from the exchange of meson trajectories  $a_0$  and  $f$ ) to the quark distribution. In the gluon distribution we neglect this term since the reggeon is expected to be constituted of quarks. Moreover, we expect that the pomeron, having vacuum quantum numbers, does not distinguish between quark flavours, i. e., the pomeron decouples from the  $T$  distribution. In contrast, the  $\Sigma$  distribution contains a pomeron and a reggeon component. The initial distributions, thus, read

$$\begin{aligned} T(x, Q_0^2) &= \tau x^{\alpha_0} (1-x)^\sigma, \\ \Sigma(x, Q_0^2) &= [a \ln(1/x) + b + dx^{\alpha_0}] (1-x)^\kappa \end{aligned} \quad (34)$$

with the reggeon intercept  $\alpha_0 = 0.4$  and the powers  $\sigma = 3$  and  $\kappa = 2$  of  $(1-x)$  taking into account daughter trajectories in Regge theory. For  $x > x_{\text{GRV}}$ , we again rely on the GRV distributions since our  $T$  and  $\Sigma$  distributions are only valid at small  $x$ . The parameters  $\tau$  and  $b$  are fixed to ensure continuity between our distributions and GRV's ones at  $x = x_{\text{GRV}}$ . Finally, we are left with 2 parameters,  $a$  and  $d$ , which we determine by fitting the  $F_2^p(x, Q^2)$  experimental data.

## V. RESULTS

With the previous  $T$ ,  $\Sigma$  and  $G$  distributions at  $Q_0^2 = 1.8 \text{ GeV}^2$  as an initial condition in the DGLAP equation, we have fitted the  $F_2^p$  experimental data within the do-

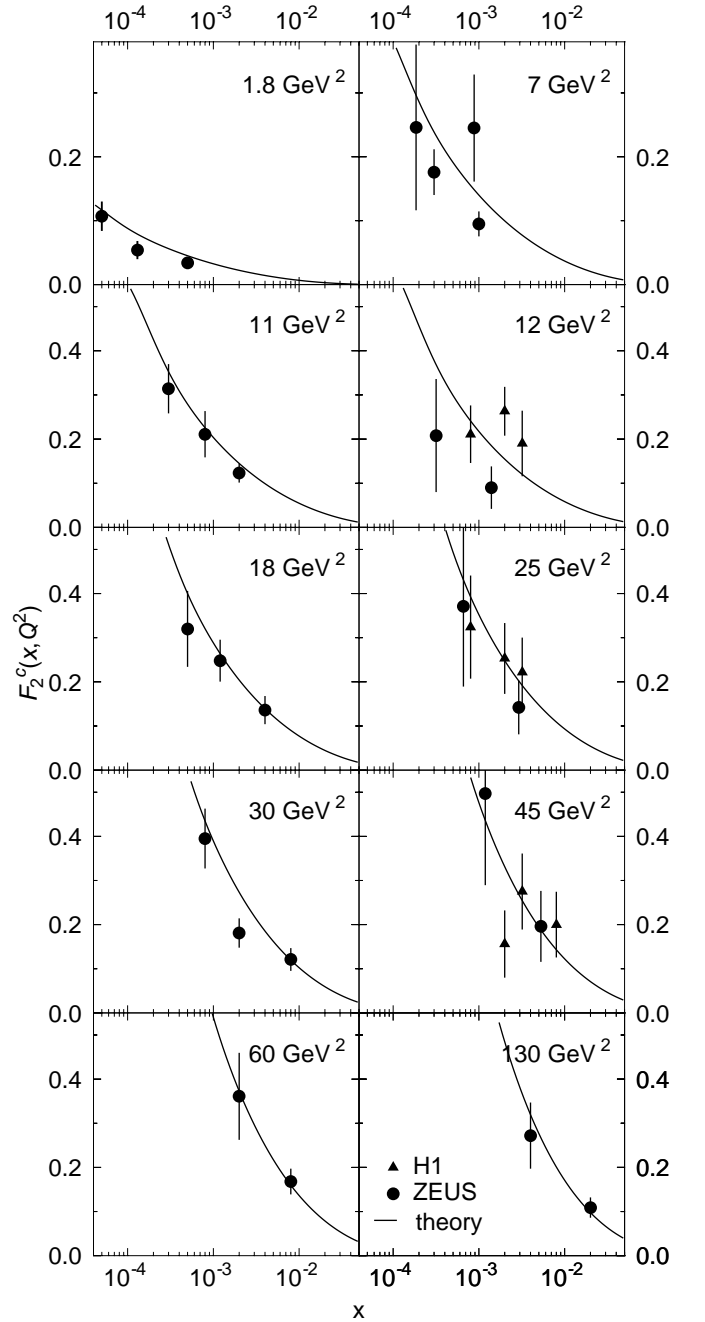


FIG. 7: The charm structure function,  $F_2^c(x, Q^2)$ , as a function of the Bjorken-variable  $x$  at different virtualities  $Q^2$ .

main

$$\begin{aligned} Q^2 &\geq Q_0^2 = 1.8 \text{ GeV}^2, \\ x &\leq x_{\text{GRV}} = 0.15, \\ \cos(\theta_t) &= \frac{\sqrt{Q^2}}{2x m_p} \geq \frac{49 \text{ GeV}^2}{2m_p^2}. \end{aligned} \quad (35)$$

Here  $m_p$  denotes the proton mass,  $\theta_t$  is the scattering angle in the  $t$ -channel and  $\cos(\theta_t)$  has been extended to the whole complex plane. The last condition of  $\cos(\theta_t)$



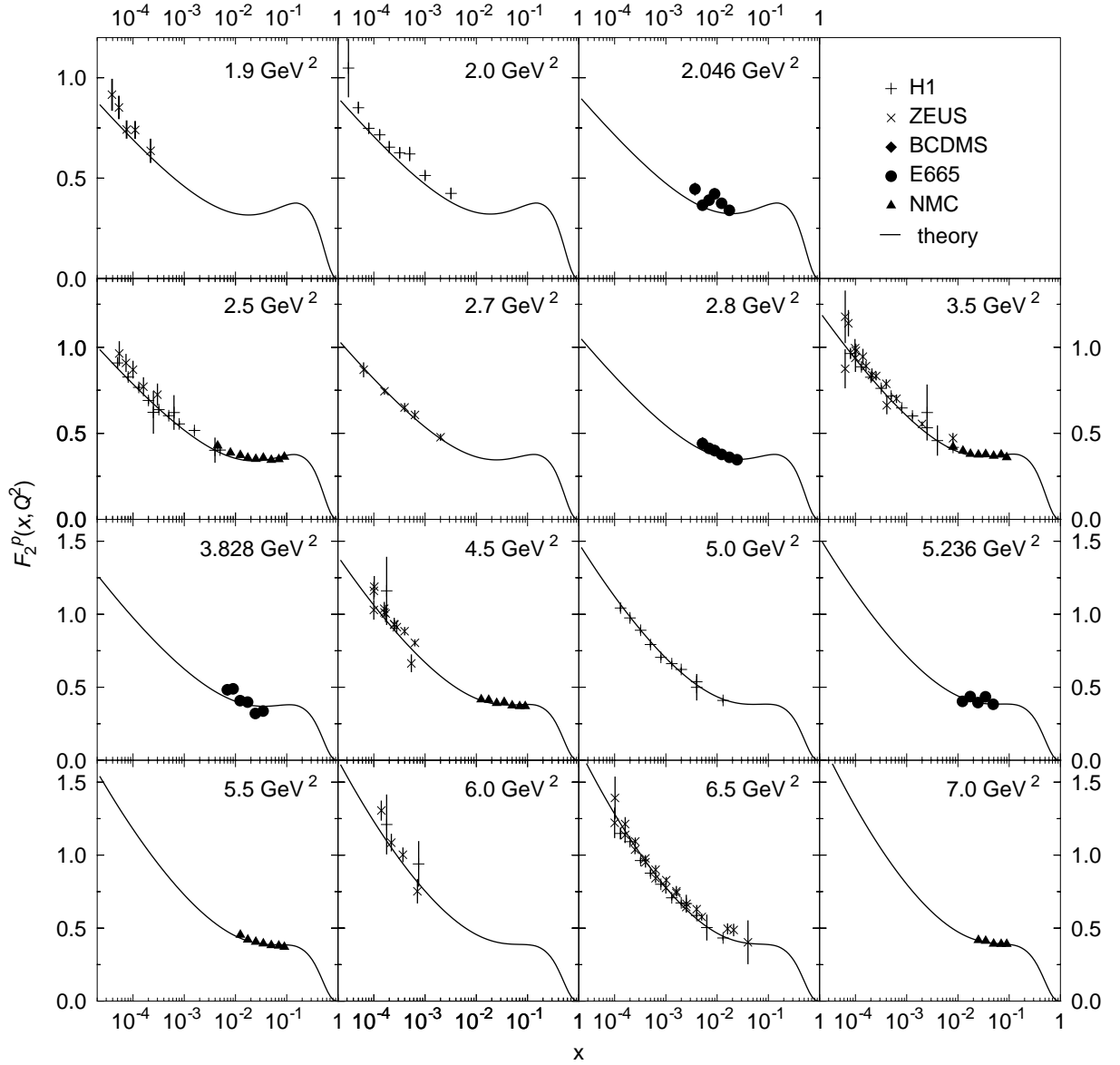


FIG. 8: The proton structure function,  $F_2^p(x, Q^2)$ , as a function of the Bjorken-variable  $x$  at low virtualities  $Q^2$ .

taken from [26] ensures that Regge theory is applicable. We have used 922 experimental points coming from H1 [27, 28, 29], ZEUS [30, 31], BCDMS [32], E665 [33] and NMC [34] to adjust our parameters within the given region. We have obtained the following values

$$\begin{aligned}
 a &= 0.45933 \pm 0.00425, \\
 b &= -1.9598 \quad (\text{fixed by continuity}), \\
 d &= 6.0408 \pm 0.0456, \\
 \tau &= 0.55628 \quad (\text{fixed by continuity}).
 \end{aligned}$$

In Figs. 8, 9 and 10 we show the results for the proton structure function,  $F_2^p(x, Q^2)$ , as a function of the Bjorken-variable  $x$  between the virtualities  $Q^2 =$

$1.8 \text{ GeV}^2$  and  $Q^2 = 3000 \text{ GeV}^2$ . Our results are in good agreement with experimental data for all  $x$  and  $Q^2$  values.

To test our gluon distribution, we compute the charm structure function which depends on the gluon distribution as follows [35]

$$F_2^c(x, Q^2) = 2e_c^2 \frac{\alpha_s(Q^2 + 4m_c^2)}{2\pi} \int_{ax}^1 d\xi g(\xi, Q^2 + 4m_c^2) f(x/\xi, Q^2),$$

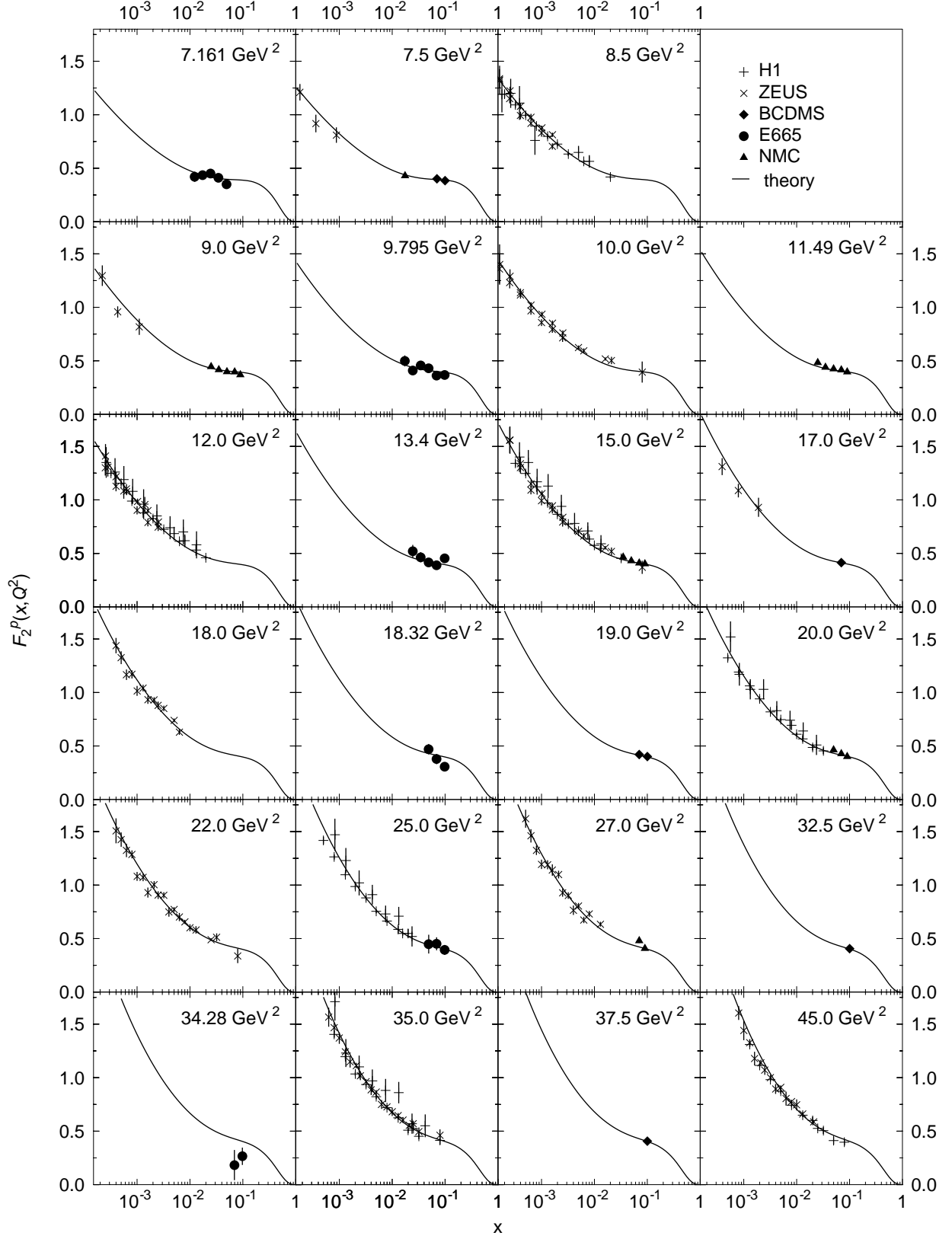


FIG. 9: The proton structure function,  $F_2^p(x, Q^2)$ , as a function of the Bjorken-variable  $x$  at middle-range virtualities  $Q^2$ .

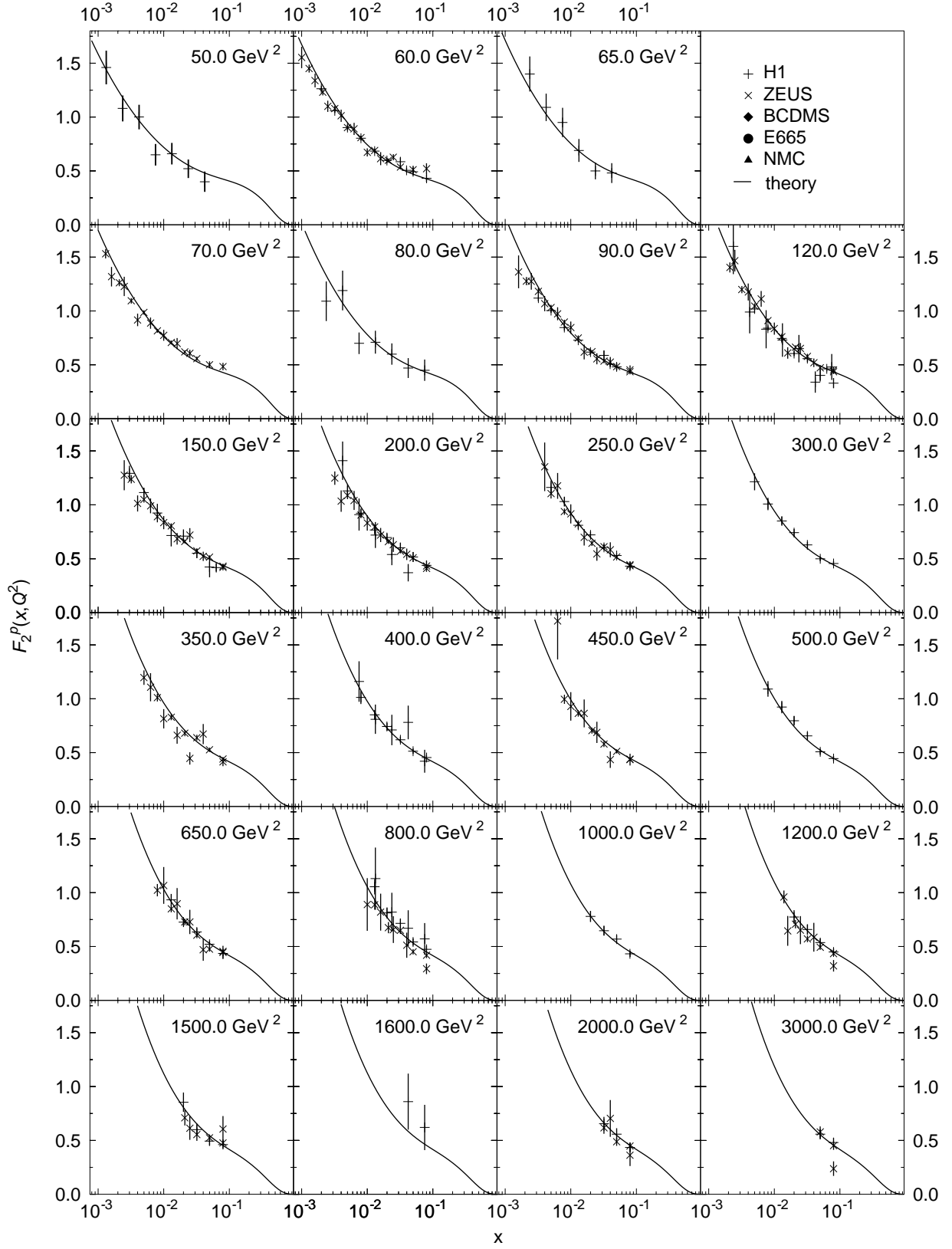


FIG. 10: The proton structure function,  $F_2^p(x, Q^2)$ , as a function of the Bjorken-variable  $x$  at high virtualities  $Q^2$ .

with

$$\begin{aligned}
f(x, Q^2) &= v \left[ (4 - \mu)x^2(1 - x) - \frac{x}{2} \right] \\
&+ L \left[ \frac{x}{2} - x^2(1 - x) + \mu x^2(1 - 3x) - \mu^2 x^3 \right], \\
\mu &= \frac{2m_c^2}{Q^2}, \\
v &= \sqrt{1 - \frac{2x\mu}{1 - x}}, \\
L &= \log \left( \frac{1 + v}{1 - v} \right), \\
a &= 1 + 2\mu.
\end{aligned}$$

We have adopted a value of 1.25 GeV for the charm quark mass. The predictions for  $F_2^c(x, Q^2)$  obtained from our model are presented together with the experimental HERA data [30, 36, 37] in Fig. 7. The good agreement of our predictions for  $F_2^c(x, Q^2)$  with experimental data clearly shows that we obtain a reasonable gluon distribution.

## VI. CONCLUSIONS

We have considered the interaction of a scalar “photon”, which directly couples to the gluons, with an external color field to extract the leading and next-to-leading order gluon distribution. We have closely followed the previous work by Dosch, Hebecker, Metz and Pirner [1], in which the semiclassical approach (where the partonic fluctuations of the “photon” interact with the proton in the eikonal approximation) has been compared with the

parton model to get the gluon distribution of the proton. The leading order result is a constant while the next-to-leading order result has a  $\ln(1/x)$  rise at small  $x$ .

We have been able to relate the leading and next-to-leading order gluon distribution to the short and long distance behavior of the cross section of a dipole in the adjoint representation of  $SU(3)$  scattering off a proton, respectively. In addition, a gluon mass has been introduced to take into account nonperturbative effects in the small- $k_\perp$  region of the perturbatively derived wave function of the two gluons emerging from the scalar “photon”, in analogy to the constituent quark mass in the quark-antiquark wave function. We have computed the adjoint dipole-proton cross section in the loop-loop correlation model [3] to obtain numerical results for the gluon distributions at the initial scale  $Q_0^2 = 1.8 \text{ GeV}^2$ .

Quark distributions at the same initial scale have been parametrized in line with Regge theory and the ideas leading to the gluon distribution. We have used DGLAP equations to evolve quark and gluon distributions to higher  $Q^2$  values. The charm and proton structure functions computed in the small- $x$  region are in good agreement with experimental HERA data over a large range of  $Q^2$  values.

## Acknowledgments

We would like to thank Arthur Hebecker and Stephane Munier for stimulating discussions. This research is partially funded by the INTAS project “Non-Perturbative QCD” and the European TMR Contract HPRN-CT-2000-00130. G. S. is supported by the National Fund for Scientific Research (FNRS), Belgium.

- 
- [1] H. G. Dosch, A. Hebecker, A. Metz and H. J. Pirner, Nucl. Phys. B **568** (2000) 287.
  - [2] A. H. Mueller, Nucl. Phys. B **335** (1990) 115.
  - [3] A. I. Shoshi, F. D. Steffen and H. J. Pirner, Nucl. Phys. A **709** (2002) 131.
  - [4] O. Nachtmann, Annals Phys. **209** (1991) 436.
  - [5] O. Nachtmann, in “Perturbative and Nonperturbative Aspects of Quantum Field Theory,” edited by H. Latal and W. Schweiger (Springer Verlag, Berlin, Heidelberg 1997) [hep-ph/9609365].
  - [6] A. Krämer and H. G. Dosch, Phys. Lett. B **252** (1990) 669.
  - [7] H. G. Dosch, E. Ferreira and A. Krämer, Phys. Rev. D **50** (1994) 1992.
  - [8] T. Regge, Nuovo Cim. **14**, 951 (1959);  
T. Regge, Nuovo Cim. **18**, 947 (1960);  
See for a modern overview of Regge theory and diffraction the books *Pomeron Physics and QCD* by S. Donnachie, G. Dosch, P. Landshoff and O. Nachtmann (Cambridge University Press, Cambridge, 2002), and *High-Energy Particle Diffraction* by V. Barone and E. Predazzi (Springer, Berlin, Heidelberg, 2002).
  - [9] V. N. Gribov and L. N. Lipatov, Yad. Fiz. **15** (1972) 781;
  - L. N. Lipatov, Sov. J. Nucl. Phys. **20** (1975) 94;  
G. Altarelli and G. Parisi, Nucl. Phys. B **126** (1977) 298;  
Y. L. Dokshitzer, Sov. Phys. JETP **46** (1977) 641.
  - [10] M. Haas, “Berechnung der Gluonverteilung des Protons unter Benutzung zweier nichtperturbativer Modelle,” Diploma Thesis, Heidelberg 2000.
  - [11] H. G. Dosch, T. Gousset and H. J. Pirner, Phys. Rev. D **57** (1998) 1666.
  - [12] W. Buchmüller, T. Gehrmann and A. Hebecker, Nucl. Phys. B **537** (1999) 477.
  - [13] A. I. Shoshi, “Anatomy of QCD strings and saturation effects in high-energy scattering,” arXiv:hep-ph/0302179.
  - [14] A. I. Shoshi, F. D. Steffen, H. G. Dosch and H. J. Pirner, Phys. Rev. D **66** (2002) 094019.
  - [15] A. I. Shoshi, F. D. Steffen, H. G. Dosch and H. J. Pirner, Phys. Rev. D **68** (2003) 074004.
  - [16] F. D. Steffen, “From static potentials to high-energy scattering,” arXiv:hep-ph/0301084.
  - [17] D. Kharzeev, Phys. Lett. B **378** (1996) 238.
  - [18] F. J. Wegner, J. Math. Phys. **12** (1971) 2259;  
K. G. Wilson, Phys. Rev. D **10** (1974) 2445.
  - [19] H. G. Dosch, T. Gousset, G. Kulzinger and H. J. Pirner, Phys. Rev. D **55** (1997) 2602.

- [20] M. Wirbel, B. Stech and M. Bauer, *Z. Phys. C* **29** (1985) 637.
- [21] L. Del Debbio, A. Di Giacomo and Y. A. Simonov, *Phys. Lett. B* **332** (1994) 111.
- [22] M. Rueter and H. G. Dosch, *Z. Phys. C* **66** (1995) 245.
- [23] A. I. Shoshi and F. D. Steffen, “Saturation effects in hadronic cross sections,” arXiv:hep-ph/0212070; A. I. Shoshi, F. D. Steffen and H. J. Pirner, “Gluon saturation and S-matrix unitarity,” arXiv:hep-ph/0205343.
- [24] M. Gluck, E. Reya and A. Vogt, *Eur. Phys. J. C* **5**, 461 (1998).
- [25] G. Soyez, *Phys. Rev. D* **67** (2003) 076001.
- [26] J. R. Cudell, E. Martynov and G. Soyez, “t-channel unitarity and photon cross sections,” arXiv:hep-ph/0207196.
- [27] C. Adloff *et al.* [H1 Collaboration], *Eur. Phys. J. C* **13**, 609 (2000).
- [28] C. Adloff *et al.* [H1 Collaboration], *Eur. Phys. J. C* **19**, 269 (2001).
- [29] C. Adloff *et al.* [H1 Collaboration], *Eur. Phys. J. C* **21**, 33 (2001).
- [30] J. Breitweg *et al.* [ZEUS Collaboration], *Eur. Phys. J. C* **12**, 35 (2000).
- [31] S. Chekanov *et al.* [ZEUS Collaboration], *Eur. Phys. J. C* **21**, 443 (2001).
- [32] A. C. Benvenuti *et al.* [BCDMS Collaboration], *Phys. Lett. B* **223**, 485 (1989).
- [33] M. R. Adams *et al.* [E665 Collaboration], *Phys. Rev. D* **54**, 3006 (1996).
- [34] NMC Collaboration: M. Arneodo *et al.*, *Nucl. Phys. B* **483** (1997) 3; *Nucl. Phys. B* **487** (1997) 3.
- [35] R.G. Roberts, *The Structure of the Proton*, Cambridge University Press (1990).
- [36] C. Adloff *et al.* [H1 Collaboration], *Z. Phys. C* **72**, 593 (1996).
- [37] J. Breitweg *et al.* [ZEUS Collaboration], *Phys. Lett. B* **407**, 402 (1997).
- [38] Note that the expressions “LO” and “NLO” gluon distribution do not refer to the order of expansion of the splitting functions in DGLAP evolution. LO (resp. NLO) distribution corresponds to one (resp. two) gluon(s) in the final state, calculated in the large- $Q^2$  and small- $x$  limit.
- [39] The proton has in fact a three-quark structure and is described by three dipoles [7, 17] instead of a quark-diquark dipole as done here. However the quark-diquark description simplifies enormously the model and gives similar results as the three-dipole picture once the model parameters are readjusted [7].

# Log( $1/x$ ) Gluon Distribution and Structure Functions in the Loop-Loop Correlation Model

H. J. Pirner<sup>1,\*</sup>, A. I. Shoshi<sup>1,†</sup>, and G. Soyez<sup>2,‡</sup>

<sup>1</sup>*Institut für Theoretische Physik, Universität Heidelberg,  
Philosophenweg 19, D-69120 Heidelberg, Germany*

<sup>2</sup>*Inst. de Physique, Bât. B5, Université de Liège,  
Sart-Tilman, B4000 Liège, Belgium*

We consider the interaction of the partonic fluctuation of a scalar “photon” with an external color field to calculate the leading and next-to-leading order gluon distribution of the proton following the work done by Dosch-Hebecker-Metz-Pirner [1]. We relate these gluon distributions to the short and long distance behavior of the cross section of an adjoint dipole scattering off a proton. The leading order result is a constant while the next-to-leading order result shows a  $\ln(1/x)$  enhancement at small  $x$ . To get numerical results for the gluon distributions at the initial scale  $Q_0^2 = 1.8 \text{ GeV}^2$ , we compute the adjoint dipole-proton cross section in the loop-loop correlation model. Quark distributions at the same initial scale are parametrized according to Regge theory. We evolve quark and gluon distributions to higher  $Q^2$  values using the DGLAP equation and compute charm and proton structure functions in the small- $x$  region for different  $Q^2$  values.

Keywords: Gluon Distribution, Quark Distribution, High-Energy Scattering, Non-Perturbative QCD, DGLAP Evolution, Regge Theory, Charm Structure Function, Proton Structure Function.

PACS numbers: 11.80.Fv, 12.38.-t, 12.40.-y, 13.60.-r.

## I. INTRODUCTION

The understanding of deep inelastic scattering (DIS) in the small- $x$  regime remains one of the challenges in quantum chromodynamics (QCD). Perturbative and nonperturbative physics are important for a complete picture of the small- $x$  limit of structure functions. In this work, we combine perturbative and nonperturbative approaches to describe charm and proton structure functions (or quark and gluon distributions) in the small- $x$  region.

The basic idea is the description of high-energy scattering in QCD by studying the eikonalized interaction of energetic partons with external color fields. In ref. [1], this semiclassical method has been compared with the parton model to extract the leading order (LO) and next-to-leading order (NLO) gluon distribution. The main idea is simple and goes back to Muller [2]. One calculates the gluon production cross section for a scalar “photon”, which directly couples to the gluon field, in an external color field. The calculation of one-gluon production leads to the LO gluon distribution and the one of two-gluon production to the NLO gluon distribution. The LO result turns out to be a constant,  $xg^{(0)}(x, Q^2) \propto \text{const.}$ , characterising the averaged local field strength in the proton. The NLO result shows a logarithmic increase at small  $x$ ,  $xg^{(1)}(x, Q^2) \propto \ln(1/x)$ , and is sensitive to the large distance structure of the proton.

In order to make numerical estimates for the gluon distributions, we relate the LO and NLO gluon distributions to the scattering of a dipole in the adjoint representation of  $SU(3)$  on a proton. Then, we use the loop-loop correlation model (LLCM) [3] to compute this adjoint dipole - proton cross section at the center of mass (c.m.) energy of  $\sqrt{s_0} \approx 20 \text{ GeV}$ . The two gluons emerging from the scalar “photon” represent the adjoint dipole and a fundamental quark-diquark dipole models the proton in the LLCM. The correlation between the two dipoles given by Wegner-Wilson loops is evaluated in the Gaussian approximation of gluon field strengths. The perturbative interactions are obtained from perturbation theory and the nonperturbative gluon field strength correlator is parametrized in line with simulations in the lattice QCD. The calculation of scattering cross sections in the loop-loop correlation model has been quite successful at low energies  $\sqrt{s_0} \approx 20 \text{ GeV}$  [3–7].

For small virtuality  $Q^2$ , the perturbative wave function of the two gluons emerging from the scalar “photon” is unrealistically extended at the endpoints of the longitudinal momentum fraction  $\alpha = 0, 1$ . This problem is similar to the quark-antiquark wave function of the transverse photon. The phenomenological solution we propose is to give the gluon a constituent mass  $m_G$  of the order of the rho mass. This mass modifies the wave function at small transverse gluon momenta  $k_\perp$  ensuring “confinement” for the two gluons, but does not affect the perturbative part of the two-gluon wave function at high  $k_\perp$ .

We calculate the  $x$ -dependence of the gluon distribution at a scale  $Q_0^2 = 1.8 \text{ GeV}^2$  which corresponds to the upper limit where the nonperturbative input is still credible. The quark distributions at the same scale are

---

\*E-mail address: pir@tphys.uni-heidelberg.de

†E-mail address: shoshi@tphys.uni-heidelberg.de

‡E-mail address: g.soyez@ulg.ac.be

parametrized in line with Regge theory [8]. We evolve both distributions to higher values of  $Q^2$  using DGLAP equations [9]. With quark and gluon distributions, we compute charm and proton structure functions at small  $x$  for different  $Q^2$  values in good agreement with experimental data.

The outline of the paper is as follows: In section II we review the formulas for the calculation of the LO and NLO gluon distribution following [1], introduce a gluon mass into the formalism and rewrite the final expressions for gluon distributions in terms of adjoint dipole-proton cross sections. We compute the adjoint dipole-proton cross section in the loop-loop correlation model in section III. In section IV we determine the  $x$  dependence of the quark distributions at the initial scale  $Q_0^2$  according to Regge theory. The initial gluon and quark distributions are evolved to higher virtualities  $Q^2$  using the DGLAP equation. In section V we present the results for the charm and proton structure function versus Bjorken- $x$  at different  $Q^2$  values. Finally, in section VI, we summarize our results.

## II. THE SEMI-CLASSICAL GLUON DISTRIBUTION

In this section we review the formulas for the computation of the LO and NLO gluon distribution in the semiclassical approach and parton model following the work by Dosch, Hebecker, Metz and Pirner [1]. In addition, we introduce a gluon mass in the formalism to take into account the spatial localization of the two gluons due to confinement. We derive the modifications due to massive gluons and rewrite the final results for the gluon distributions in terms of adjoint dipole-proton cross sections.

### A. Gluon distribution at leading order

In order to extract the gluon distribution, we consider a scalar field  $\chi$  (or scalar “photon”) coupled directly to the gluon field through the interaction lagrangian

$$\mathcal{L}_I = -\frac{\lambda}{2} \chi \text{tr}(\mathbf{F}_{\mu\nu} \mathbf{F}^{\mu\nu}) ,$$

with  $\mathbf{F}_{\mu\nu} = F_{\mu\nu}^a t^a$ , the gluon field strength  $F_{\mu\nu}^a = [\partial_\mu A_\nu^a - \partial_\nu A_\mu^a - g f^{abc} A_\mu^b A_\nu^c]$ , the gluon field  $A^a$  and the  $SU(N_c)$  group generators in the adjoint representation  $t^a$ . In the high-energy limit, the scattering of a  $\chi$ -particle off an external color field  $A^a$  as shown in Fig. 1(a), has the following amplitude

$$\mathcal{T}^a(b_\perp) = \frac{i\lambda q_0}{2C_A} \int dx_+ \text{tr} [t^a (\epsilon_\perp^* \partial_\perp) A_-^A(x_+, b_\perp)] .$$

Here  $b_\perp$  denotes the impact parameter in transverse space,  $q$  the four momentum vector of the  $\chi$ -particle,  $x_+ = x_0 + x_3$  the light-cone variable,  $\partial_\perp \equiv \partial/\partial b_\perp$ ,

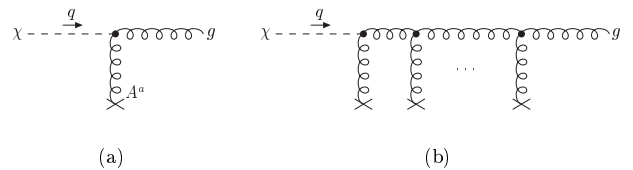


FIG. 1: The process  $\chi \rightarrow g$  in an external color field: (a) one gluon exchange, (b) resummed gluon exchange.

$A^A = A^b t^b$  the external color field,  $C_A = N_c$  the Casimir operator in the adjoint representation,  $N_c$  the number of colors and  $\epsilon_\perp$  the polarisation vector of the outgoing gluon.

Resumming the gluon exchange to all orders as shown in Fig. 1(b), the gluon initially created at the vertex  $\chi gg$  acquires a non-abelian eikonal factor on the way through the external color field

$$U_{(\infty, x_+)}^A(b_\perp) = P \exp \left[ -\frac{ig}{2} \int_{x_+}^{\infty} dx_+ A_-^A(x_+, b_\perp) \right] .$$

The path ordering along the way  $x_+$  is denoted by  $P$ . With

$$W_{b_\perp}^A(r_A) = U^A(b_\perp - r_A/2) U^{A\dagger}(b_\perp + r_A/2) - \mathbb{1} , \quad (1)$$

where the eikonal factors  $U^A(b_\perp - r_A/2) \equiv U_{\infty, -\infty}^A(b_\perp - r_A/2)$  and  $U^{A\dagger}(b_\perp + r_A/2)$  come from the scattering of two gluons (moving in opposite directions) with transverse distance  $r_A$  off the proton, the semiclassical (sc) cross-section for gluon production at leading order becomes (cf. ref. [1])

$$\sigma_{\text{sc}}^{(0)} = \frac{\lambda^2}{4g^2 C_A} \int d^2 b_\perp \left| [\partial_{r_A} W_{b_\perp}^A(r_A)]_{r_A=0} \right|^2 . \quad (2)$$

In the following an average over the external color fields underlying the quantity  $W_{b_\perp}^A$  is implicitly understood.

On the other hand, the leading-order parton model (pm) cross section for the partonic process  $\chi g \rightarrow g$  shown in Fig. 2 with the proton described by the gluon distribution is given by

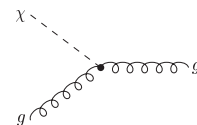


FIG. 2: The process  $\chi g \rightarrow g$  in the parton model.

bution is given by

$$\sigma_{\text{pm}}^{(0)} = \frac{\pi\lambda}{4} x g^{(0)}(x, Q^2) . \quad (3)$$

Identifying the semiclassical cross-section (2) with the partonic one (3), one finds the leading-order gluon dis-

tribution

$$xg^{(0)}(x, Q^2) = \frac{1}{2\pi^2\alpha_s} \frac{1}{2C_A} \int d^2b_\perp \left| [\partial_{r_A} W_{b_\perp}^A(r_A)]_{r_A=0} \right|^2. \quad (4)$$

Using the expression for the adjoint dipole (d) - proton (p) cross section in the semiclassical approach [1, 11]

$$\sigma_{sc}^{dp}(r_A) = -\frac{2}{3} \int d^2b_\perp \text{tr} W_{b_\perp}^A(r_A) \quad (5)$$

and the identity

$$\int d^2b_\perp \left| [\partial_{r_A} W_{b_\perp}^A(r_A)]_{r_A=0} \right|^2 = - \left[ \partial_{r_A}^2 \int d^2b_\perp \text{tr} W_{b_\perp}^A(r_A) \right]_{r_A=0} \quad (6)$$

one can rewrite eq. (4) in the useful form

$$xg^{(0)}(x, Q^2) = \frac{3}{4\pi^2\alpha_s} \frac{1}{2C_A} [\partial_{r_A}^2 \sigma_{sc}^{dp}(r_A)]_{r_A=0}. \quad (7)$$

This equation shows that the LO gluon distribution depends on the small distance behavior of the adjoint dipole-proton cross section. To get numerical results for the gluon distribution, we use in the next section a model to compute the adjoint dipole-proton cross section.

## B. Gluon distribution at next-to-leading order

For the semiclassical calculation of the gluon distribution at next-to-leading order, the three diagrams shown in Fig. 3 are relevant in the high energy limit. Resumming the interaction with the external field to all orders, i. e., repeating the step leading from Fig. 1(a) to Fig. 1(b), we obtain the result shown in Fig. 4. In the first diagram the incoming  $\chi$ -particle splits into two gluons before interacting with the target. The subsequent scattering of the two gluons off the external color field is treated in the eikonal approximation. In the second diagram the two fast gluons are created through a  $\chi ggg$  vertex in the space-time region of the external color field.

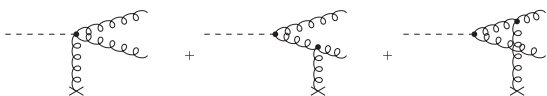


FIG. 3: Diagrams contributing to the  $\chi \rightarrow gg$  amplitude in the high-energy limit.



FIG. 4: Relevant contributions in the NLO semiclassical calculation.

One can show [1] that the amplitudes in Fig. 4 produce the following NLO contribution to the cross-section

$$\sigma_{sc}^{(1)}(x, Q^2) = \frac{\lambda^2}{32(2\pi)^6} \int \frac{d\alpha}{\alpha(1-\alpha)} \int dk_\perp'^2 \int d^2b_\perp \left| \int d^2k_\perp \frac{N^2 \delta_{ij} + 2k_i k_j}{N^2 + k_\perp^2 + m_G^2} \tilde{W}_{b_\perp}^A(k'_\perp - k_\perp) \right|^2, \quad (8)$$

where  $\alpha$  and  $1-\alpha$  are the longitudinal momentum carried by the two gluons,  $k_\perp$  and  $k'_\perp$  are the transverse momenta of one of the two gluons before and after the interaction with the external field,  $N^2 = \alpha(1-\alpha)Q^2$  and  $\tilde{W}_{b_\perp}^A(k_\perp)$  is the Fourier transform of  $W_{b_\perp}^A(r_A)$  given in eq. (1).

In equation (8) we have introduced a gluon mass  $m_G$  into the gluon propagator. This mass mimics the confinement of the two gluons emerging from the  $\chi$ -particle and modifies their perturbative wave function in the non-perturbative, small  $k_\perp$  region for small virtualities  $Q^2$  or momentum fractions  $\alpha = 0, 1$ . Phenomenologically, the gluon mass has a similar effect as a constituent quark mass in the perturbative quark-antiquark wave function of the transverse photon [10]. We use for the gluon mass  $m_G = 770$  MeV, i.e., approximately half of the glueball mass.

To compute the NLO contribution to the gluon distribution in the parton model, we have to calculate the diagrams shown in Fig. 5. With  $z = Q^2/(Q^2 + s) = x/y$ ,

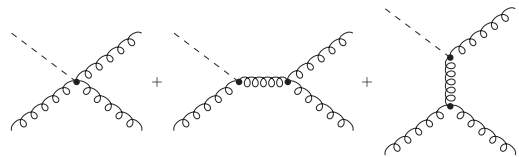


FIG. 5: Diagrams contributing to the parton model at NLO.

where  $y$  is the fraction of the target momentum carried by the struck gluon, the parton model cross-section at NLO reads

$$\sigma_{pm}(x, Q^2) = \int_x^1 \frac{dz}{z} \left[ \sigma_d^{(0)} \delta(1-x) + \hat{\sigma}^{(1)}(x, Q^2) \right] yg_b(y), \quad (9)$$

with  $\sigma_d^{(0)} = (\pi\lambda_d^2)/4$  and the  $d = (4 + \varepsilon)$  dimensional coupling  $\lambda_d = \lambda\mu^{-\varepsilon/2}$ . Since we are interested in the high energy limit, we extract only the leading term in  $\ln(1/x)$  from the expression in (9). We regularize the bare gluon distribution  $g_b(x)$  in the  $\overline{\text{MS}}$  scheme

$$g_b(x) = g(x, \mu^2) - \frac{\alpha_s}{2\pi} \int_x^1 \frac{dz}{z} P_{gg}(z) \left[ \frac{2}{\varepsilon} + \gamma_E - \ln(4\pi) \right] g(y, \mu^2),$$

with  $P_{gg}$  denoting the gluon-gluon splitting function.



The parton model cross-section at NLO finally becomes

$$\sigma_{\text{pm}} = \sigma_{d=4}^{(0)} x \int_x^1 \frac{dz}{z} g(y, \mu^2) \left\{ \delta(1-z) + \frac{\alpha_s}{2\pi} \left[ P_{gg}(z) \ln \left( \frac{Q^2}{\mu^2} \right) + C_g^{\overline{\text{MS}}}(z) \right] \right\}, \quad (10)$$

where

$$C_g^{\overline{\text{MS}}}(z) = P_{gg}(z) \ln \left( \frac{1-z}{z} \right) - \frac{11C_A}{6z(1-z)}.$$

Expanding the full gluon distribution up to the order  $\ln(1/x)$

$$xg(x, \mu^2) = xg^{(0)}(x, \mu^2) + xg^{(1)}(x, \mu^2),$$

and identifying (8) with (10), we obtain

$$\begin{aligned} xg^{(1)}(x, \mu^2) &= \frac{1}{4(2\pi)^7} \int \frac{d\alpha}{\alpha(1-\alpha)} \int dk_{\perp}'^2 \int d^2 b_{\perp} \\ &\times \left| \int d^2 k_{\perp} \frac{N^2 \delta_{ij} + 2k_i k_j}{N^2 + k_{\perp}^2 + m_G^2} \tilde{W}_{b_{\perp}}^A(k'_{\perp} - k_{\perp}) \right|^2 \\ &- \frac{\alpha_s}{2\pi} \int_x^1 dz \left[ P_{gg}(z) \ln \left( \frac{Q^2}{\mu^2} \right) + C_g^{\overline{\text{MS}}}(z) \right] yg^{(0)}(y, \mu^2), \end{aligned} \quad (11)$$

where  $g^{(0)}(x, \mu^2)$  is given by (4). When evaluating equation (11), we keep only  $\ln(1/x)$  terms, i.e., we use

$$\begin{aligned} P_{gg}(z) &\approx \frac{2C_A}{z}, \\ C_g^{\overline{\text{MS}}}(z) &\approx \frac{2C_A}{z} \left[ \ln \left( \frac{1}{z} \right) - \frac{11}{12} \right]. \end{aligned}$$

Using the variable  $z = Q^2/(Q^2 + M^2)$ , with  $M^2 = k_{\perp}'^2/(\alpha(1-\alpha))$ , and introducing a scale  $\kappa^2$  such that  $\Lambda_{QCD}^2 \ll \kappa^2 \ll Q^2$ , the first contribution in (11) can be split into a hard and a soft component [1, 11]

$$\begin{aligned} &\frac{1}{4(2\pi)^7} \int \frac{d\alpha}{\alpha(1-\alpha)} \int dk_{\perp}'^2 \int d^2 b_{\perp} \\ &\times \left| \int d^2 k_{\perp} \frac{N^2 \delta_{ij} + 2k_i k_j}{N^2 + k_{\perp}^2 + m_G^2} \tilde{W}_{b_{\perp}}^A(k'_{\perp} - k_{\perp}) \right|^2 \\ &= \frac{1}{4\pi^3} \int_x^1 \frac{dz}{z} \ln \left( \frac{Q^2}{z\kappa^2} \right) \int d^2 b_{\perp} \left| [\partial_{r_A} W_{b_{\perp}}^A(r_A)]_{r_A=0} \right|^2 \\ &+ \frac{2}{\pi} \int_x^1 \frac{dz}{z} \int_0^{\kappa^2} dk_{\perp}'^2 f(k_{\perp}'^2), \end{aligned} \quad (12)$$

where

$$\begin{aligned} f(k_{\perp}'^2) &= \int \frac{d^2 r_A}{(2\pi)^2 r_A^2} \int \frac{d^2 r_A'}{(2\pi)^2 r_A'^2} \int d^2 b_{\perp} \\ &\text{tr} \left[ W_{b_{\perp}}^A(r_A) W_{b_{\perp}}^{A\dagger}(r_A') \right] e^{ik_{\perp}' \cdot (r_A - r_A')} H(r_A, r_A'), \\ H &= \frac{(r_A \cdot r_A')^2}{r_A^2 r_A'^2} [\hat{a}^2 K_0(\hat{a})] [\hat{b}^2 K_0(\hat{b})] \\ &+ \frac{1}{2} \left[ \frac{2(r_A \cdot r_A')^2}{r_A^2 r_A'^2} - 1 \right] \left\{ [\hat{a} K_1(\hat{a})] [\hat{b} K_1(\hat{b})] \right. \\ &\quad \left. + [\hat{a} K_1(\hat{a})] [\hat{b}^2 K_0(\hat{b})] \right. \\ &\quad \left. + [\hat{a}^2 K_0(\hat{a})] [\hat{b} K_1(\hat{b})] \right\}, \end{aligned}$$

with  $\hat{a} = m_G r_A$  and  $\hat{b} = m_G r_A'$ . Note that the gluon mass does not influence the hard part which is calculated at leading twist. The lower bound of the  $z$  integration,  $x \leq z$ , is a kinematical limit ensuring that the invariant mass of the two produced gluons cannot be larger than the total center-of-mass energy available [1, 11].

Inserting (12) in (11), the  $\ln^2(1/x)$  terms from the semiclassical and the parton calculations cancel, so that

$$\begin{aligned} xg^{(1)}(x, \mu^2) &= \ln \left( \frac{1}{x} \right) \left\{ \frac{2}{\pi} \int_0^{\kappa^2} dk_{\perp}'^2 f(k_{\perp}'^2) \right. \\ &\quad \left. + \frac{\alpha_s}{\pi} C_A \left[ \ln \left( \frac{\kappa^2}{\mu^2} \right) + \frac{11}{12} \right] xg^{(0)} \right\}. \end{aligned}$$

For  $\kappa^2 = \mu^2 \exp(11/12)$ , the second term also drops out and one obtains

$$xg^{(1)}(x, \mu^2) = \frac{2}{\pi} \ln \left( \frac{1}{x} \right) \int_0^{e^{11/12} \mu^2} dk_{\perp}'^2 f(k_{\perp}'^2). \quad (13)$$

After the integration over  $k_{\perp}'^2$  and  $r_A'$ , the NLO correction to the gluon distribution becomes [1, 11]

$$\begin{aligned} xg^{(1)}(x, \mu^2) &= \frac{1}{2\pi^3} \ln \left( \frac{1}{x} \right) \int_{r_0^2(\mu^2)}^{\infty} \frac{dr_A^2}{r_A^2} m_G^2 F(m_G r_A) \\ &\times \int d^2 b_{\perp} \text{tr} \left[ W_{b_{\perp}}^A(r_A) W_{b_{\perp}}^{A\dagger}(r_A) \right] \end{aligned} \quad (14)$$

where

$$\begin{aligned} r_0^2(\mu^2) &= \frac{4e^{\frac{1}{12}-2\gamma_E}}{\mu^2}, \\ F(z) &= K_1^2(z) + zK_0(z)K_1(z) + \frac{z^2}{2}K_0^2(z) \\ &= \frac{z^2}{2}K_2^2(z) - zK_1(z)K_2(z) + K_1^2(z). \end{aligned}$$

In the large- $N_c$  limit [12], one obtains the relation

$$\int d^2 b_{\perp} \text{tr} \left[ W_{b_{\perp}}^A(r_A) W_{b_{\perp}}^{A\dagger}(r_A) \right] = -2 \int d^2 b_{\perp} \text{tr} W_{b_{\perp}}^A(r_A)$$

which allows us to rewrite the NLO correction in terms of the dipole-proton cross section (5)

$$xg^{(1)}(x, \mu^2) = \ln\left(\frac{1}{x}\right) \frac{3m_G^2}{2\pi^2} \int_{r_0^2(\mu^2)}^{\infty} \frac{dr_A^2}{r_A^2} F(m_G r_A) \sigma_{sc}^{dp}(r_A). \quad (15)$$

The NLO gluon distribution depends on the large distance behavior of the adjoint dipole-proton cross section. To obtain numerical results for the LO and NLO gluon distribution, we calculate the dipole-proton cross section at some low c.m. energy  $\sqrt{s_0}$  within the loop-loop correlation model in the following section.

### III. DIPOLE-PROTON CROSS SECTION FROM THE LOOP-LOOP CORRELATION MODEL

In this section we use the loop-loop correlation model (LLCM) [3] to compute the cross section of an adjoint dipole scattering off a proton,  $\sigma_{sc}^{dp}(r_A, s_0)$ , at the c.m. energy  $\sqrt{s_0} = 20$  GeV. Then, we insert the resulting dipole-proton cross section in eqs. (7) and (15) to calculate the LO and NLO gluon distributions.

The loop-loop correlation model is based on the functional integral approach to high-energy scattering in the eikonal approximation [4–7]. Its central elements are gauge-invariant Wegner-Wilson loops. With a phenomenological energy dependence, we have shown that the LLCM allows a unified description of high-energy hadron-hadron, photon-hadron, and photon-photon reactions [3, 13] and of static properties of hadrons [14] in agreement with experimental and lattice data. In this work, we do not need a phenomenological parametrization for the energy dependence since this is generated by the formalism outlined in the sections before.

In the framework of LLCM the adjoint dipole - proton cross section reads [3, 15]

$$\sigma_{LLCM}^{dp}(r_A, s_0) = 2 \int d^2 b_{\perp} \int \frac{d\phi_A}{2\pi} \int d^2 r_{\mathcal{F}} dz_q |\psi_p(z_q, \vec{r}_{\mathcal{F}})|^2 \times \left(1 - S^{\mathcal{A}\mathcal{F}}(s_0, \vec{b}_{\perp}, \vec{r}_A, z_q, \vec{r}_{\mathcal{F}})\right). \quad (16)$$

Here the correlation of two light-like Wegner-Wilson loops

$$S^{\mathcal{A}\mathcal{F}}(s_0, \vec{b}_{\perp}, \vec{r}_A, z_q, \vec{r}_{\mathcal{F}}) = \frac{\langle \mathcal{W}^{\mathcal{A}}[C_g] \mathcal{W}^{\mathcal{F}}[C_q] \rangle_G}{\langle \mathcal{W}^{\mathcal{A}}[C_g] \rangle_G \langle \mathcal{W}^{\mathcal{F}}[C_q] \rangle_G}, \quad (17)$$

describes the elastic scattering of a dipole in the fundamental ( $\mathcal{F}$ ) with a dipole in the adjoint ( $\mathcal{A}$ ) representation of  $SU(N_c)$ . In the present case where a  $\chi$ -particle scatters off a proton, the adjoint color-dipole is given by the two gluons in the color-singlet state emerging from the  $\chi$ -particle and the fundamental color-dipole is given in a simplified picture by a quark and diquark in the

proton. Each color-dipole is represented by a light-like Wegner-Wilson loop [16]

$$\mathcal{W}^r[C] = \tilde{\text{Tr}}_r \mathcal{P} \exp \left[ -ig \oint_C dz^\mu A_\mu^a(z) t_r^a \right],$$

where the subscript  $r$  indicates the representation of  $SU(N_c)$ ,  $\tilde{\text{Tr}}_r = \text{Tr}_r(\dots)/\text{Tr} \mathbb{1}_r$  is the normalized trace in the corresponding color-space with unit element  $\mathbb{1}_r$ , and  $A_\mu(z) = A_\mu^a(z) t_r^a$  represents the gluon field with the  $SU(N_c)$  group generators in the corresponding representation,  $t_r^a$ , that demand the path ordering indicated by  $\mathcal{P}$  on the closed path  $C$  in space-time. Physically, the Wegner-Wilson loop represents the phase factor acquired by a color-charge in the  $SU(N_c)$  representation  $r$  along the light-like trajectory  $C$  in the gluon background field.

The color-dipoles have transverse size and orientation  $\vec{r}_{\mathcal{A}\mathcal{F}}$ . The longitudinal momentum fraction of the dipole carried by the quark (gluon) is  $z_q$  ( $z_g$ ). The impact parameter between the dipoles is [17]

$$\vec{b}_{\perp} = \vec{r}_g + (1 - z_g)\vec{r}_A - \vec{r}_q - (1 - z_q)\vec{r}_{\mathcal{F}} = \vec{r}_{\mathcal{A}cm} - \vec{r}_{\mathcal{F}cm},$$

where  $\vec{r}_q$ ,  $\vec{r}_{qq}$ ,  $\vec{r}_g$ , and  $\vec{r}_{\mathcal{F}}$  are the transverse positions of the quark, diquark, gluon and the gluon moving in the opposite direction, respectively. With  $\vec{r}_{\mathcal{F}} = \vec{r}_{qq} - \vec{r}_q$  and  $\vec{r}_A = \vec{r}_g - \vec{r}_q$ , the center of light-cone momenta of the two dipoles are given by  $\vec{r}_{\mathcal{A}cm} = z_g \vec{r}_g + (1 - z_g)\vec{r}_{\mathcal{F}}$  and  $\vec{r}_{\mathcal{F}cm} = z_q \vec{r}_q + (1 - z_q)\vec{r}_{qq}$ . Figure 6 illustrates the (a) space-time and (b) transverse arrangement of the dipoles.

The QCD vacuum expectation value  $\langle \dots \rangle_G$  in the loop-loop correlation function (17) represents functional integrals [5] over gluon field configurations: the functional integration over the fermion fields has already been carried out as indicated by the subscript  $G$ . The model we use for the QCD vacuum describes only gluon dynamics and, thus, implies the quenched approximation that does not allow string breaking through dynamical quark-antiquark production.

The  $\vec{r}_{\mathcal{F}}$  and  $z_q$  distribution of the fundamental color-dipole in the proton is given by the proton wave function  $\psi_p$ . We use for the proton wave function the phenomenological Gaussian Wirbel-Stech-Bauer ansatz [18]

$$\psi_p(z_q, \vec{r}_{\mathcal{F}}) = \sqrt{\frac{z_q(1 - z_q)}{2\pi S_p^2 N_p}} e^{-(z_q - \frac{1}{2})^2 / (4\Delta z_p^2)} e^{-|\vec{r}_{\mathcal{F}}|^2 / (4S_p^2)}.$$

The constant  $N_p$  is fixed by the normalization of the wave function to unity, the extension parameter  $S_p$  is approximately given by the electromagnetic radius of the proton and the width  $\Delta z_p = w/(\sqrt{2} m_p)$  [18] is determined by the proton mass  $m_p$  and the value  $w = 0.35 - 0.5$  GeV extracted from experimental data. We adopt the values  $\Delta z_p = 0.3$  and  $S_p = 0.86$  fm which have allowed a good description of many high-energy scattering data in our previous work [3].

The computation of the loop-loop correlation for one dipole in the fundamental and the other one in the adjoint representation of  $SU(N_c)$  can be found in detail in [15].

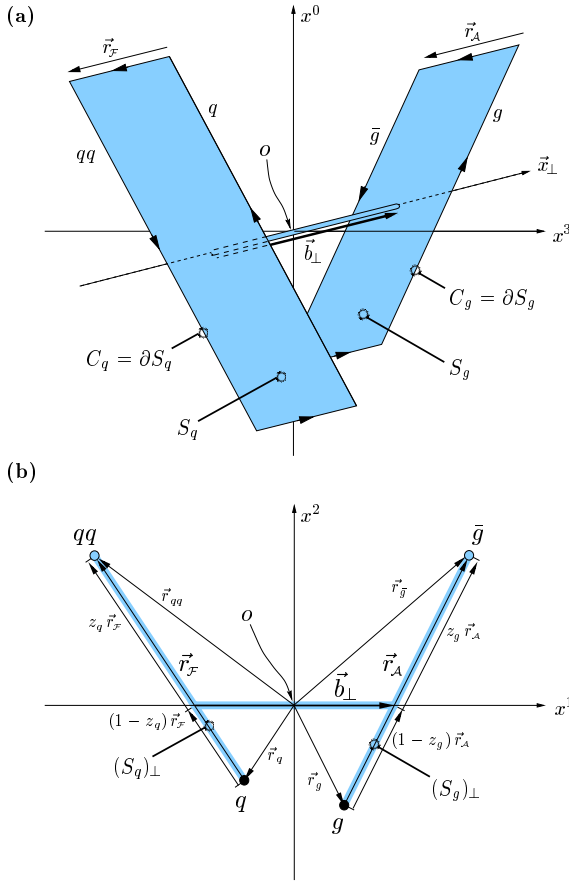


FIG. 6: High-energy scattering of a fundamental dipole with an adjoint dipole in the eikonal approximation represented by Wegner-Wilson loops: (a) space-time and (b) transverse arrangement of the Wegner-Wilson loops. The shaded areas represent the strings extending from the quark (gluon) to the diquark (antigluon) path in each color dipole. The thin tube allows to compare the field strengths in surface  $S_q$  with the field strengths in surface  $S_g$ . The impact parameter  $\vec{b}_\perp$  connects the centers of light-cone momenta of the dipoles.

The main steps of this computation are the transformation of the line integrals in the Wegner-Wilson loops into surface integrals with the non-Abelian Stokes theorem, a matrix cumulant expansion, and the Gaussian approximation of the functional integrals in the gluon field strengths. These steps lead to the following result

$$\begin{aligned} \frac{\langle \mathcal{W}^A[C_g] \mathcal{W}^F[C_q] \rangle_G}{\langle \mathcal{W}^A[C_g] \rangle_G \langle \mathcal{W}^F[C_q] \rangle_G} &= \frac{1}{N_c^2 - 1} \exp\left[i \frac{N_c}{2} \chi\right] \\ &+ \frac{N_c + 2}{2(N_c + 1)} \exp\left[-i \frac{1}{2} \chi\right] \\ &+ \frac{N_c - 2}{2(N_c - 1)} \exp\left[i \frac{1}{2} \chi\right] \quad (18) \end{aligned}$$

which, for  $N_c = 3$ , corresponds to the well-known  $SU(3)$  decomposition

$$3 \otimes 8 = 3 \oplus 15 \oplus 6.$$

The function  $\chi := \chi^P + \chi_{nc}^{NP} + \chi_c^{NP}$  has the following form [3]:

$$\begin{aligned} \chi^P &= \left[ g^2(\vec{r}_g - \vec{r}_q) iD_P'^{(2)}(\vec{r}_g - \vec{r}_q) \right. \\ &+ g^2(\vec{r}_{\bar{g}} - \vec{r}_{qq}) iD_P'^{(2)}(\vec{r}_{\bar{g}} - \vec{r}_{qq}) \\ &- g^2(\vec{r}_g - \vec{r}_{qq}) iD_P'^{(2)}(\vec{r}_g - \vec{r}_{qq}) \\ &\left. - g^2(\vec{r}_{\bar{g}} - \vec{r}_q) iD_P'^{(2)}(\vec{r}_{\bar{g}} - \vec{r}_q) \right], \quad (19) \end{aligned}$$

$$\begin{aligned} \chi_{nc}^{NP} &= \frac{\pi^2 G_2 (1 - \kappa)}{3(N_c^2 - 1)} \left[ iD_1'^{(2)}(\vec{r}_g - \vec{r}_q) + iD_1'^{(2)}(\vec{r}_{\bar{g}} - \vec{r}_{qq}) \right. \\ &\left. - iD_1'^{(2)}(\vec{r}_g - \vec{r}_{qq}) - iD_1'^{(2)}(\vec{r}_{\bar{g}} - \vec{r}_q) \right], \quad (20) \end{aligned}$$

$$\begin{aligned} \chi_c^{NP} &= \frac{\pi^2 G_2 \kappa}{3(N_c^2 - 1)} (\vec{r}_A \cdot \vec{r}_F) \\ &\times \int_0^1 dv_A \int_0^1 dv_F iD^{(2)}(\vec{r}_g + v_A \vec{r}_A - \vec{r}_q - v_F \vec{r}_F), \quad (21) \end{aligned}$$

with the perturbative ( $iD_P'^{(2)}$ ) and nonperturbative ( $iD_1'^{(2)}$  and  $iD^{(2)}(\vec{z}_\perp)$ ) correlation functions in transverse space

$$iD_P'^{(2)}(\vec{z}_\perp) = \frac{1}{2\pi} K_0(m_G |\vec{z}_\perp|), \quad (22)$$

$$iD_1'^{(2)}(\vec{z}_\perp) = \pi a^4 [3 + 3(|\vec{z}_\perp|/a) + (|\vec{z}_\perp|/a)^2] \exp(-|\vec{z}_\perp|/a), \quad (23)$$

$$iD^{(2)}(\vec{z}_\perp) = 2\pi a^2 [1 + (|\vec{z}_\perp|/a)] \exp(-|\vec{z}_\perp|/a). \quad (24)$$

We have introduced in the perturbative component  $\chi^P$  the same effective gluon mass  $m_G = 0.77 \text{ GeV}$  as before to limit the range of the perturbative interaction in the infrared region and a parameter  $M^2 = 1.04 \text{ GeV}^2$  which freezes the running coupling in the quenched approximation at the value  $g^2(\vec{z}_\perp)/(4\pi) = \alpha_s(k_\perp^2 = 0) = 0.4$  [3],

$$g^2(\vec{z}_\perp) = \frac{48\pi^2}{(33 - 2N_f) \ln \left[ (|\vec{z}_\perp|^{-2} + M^2)/\Lambda_{QCD}^2 \right]}. \quad (25)$$

In Eq. (22)  $K_0$  denotes the  $0^{th}$  modified Bessel function (McDonald function). The non-perturbative correlators (20) and (21) involve the gluon condensate  $G_2 := \langle \frac{g^2}{4\pi^2} F_{\mu\nu}^a(0) F_{\mu\nu}^a(0) \rangle = 0.074 \text{ GeV}^4$ , the parameter  $\kappa = 0.74$  that determines the relative weight of the two different components and the correlation length  $a = 0.302 \text{ fm}$  that enters through the non-perturbative correlation functions  $D$  and  $D_1$ .

The component  $\chi^P$  describes the perturbative interaction of the quark and diquark of the dipole in the proton with the two gluons of the adjoint dipole emerging from the  $\chi$ -particle as evident from (19) and Fig. 6b. The component  $\chi_{nc}^{NP}$  has the same structure as  $\chi^P$  and gives the non-perturbative interaction between the quarks and gluons of the two dipoles. The component  $\chi_c^{NP}$  shows a different structure: the integrations over  $v_A$  and  $v_F$  sum non-perturbative interactions between the strings (flux tubes) confining the quark and diquark or the two gluons in the dipoles as visualized in Fig. 6b. As shown in [14, 19, 20], the  $\chi_c^{NP}$  component leads to color-confinement due to a flux tube formation between a static quark-antiquark pair. Manifestations of confinement in high-energy scattering have been analysed in [13].

Since the squared proton wave function  $|\psi_p(z_q, \vec{r}_F)|^2$  is invariant and the  $\chi$ -function changes sign under the replacement  $(\vec{r}_F \rightarrow -\vec{r}_F, z_q \rightarrow 1 - z_q)$

$$\chi(\vec{b}_\perp, z_g, \vec{r}_A, 1 - z_q, -\vec{r}_F) = -\chi(\vec{b}_\perp, z_g, \vec{r}_A, z_q, \vec{r}_F) ,$$

only the real part of the exponentials in eq. (18) survives in the integration over  $\vec{r}_F$  and  $z_q$  so that one obtains

$$\begin{aligned} \frac{\langle \mathcal{W}^A[C_g] \mathcal{W}^F[C_q] \rangle_G}{\langle \mathcal{W}^A[C_g] \rangle_G \langle \mathcal{W}^F[C_q] \rangle_G} &= \frac{1}{N_c^2 - 1} \cos \left[ \frac{N_c}{2} \chi \right] \\ &+ \frac{N_c + 2}{2(N_c + 1)} \cos \left[ \frac{1}{2} \chi \right] \\ &+ \frac{N_c - 2}{2(N_c - 1)} \cos \left[ \frac{1}{2} \chi \right] . \end{aligned} \quad (26)$$

The above expression describes multiple gluonic interactions between two dipoles since  $(\chi^P)^2$  represents the perturbatively well-known two-gluon exchange and  $(\chi^{NP})^2$  the non-perturbative two-point interaction in the dipole-dipole scattering [13]. The higher order terms in the expansion of the cosine functions ensure the  $S$ -matrix unitarity condition which becomes important at very high c.m. energies [3, 15, 21].

The adjoint dipole-proton cross section obtained with the above ingredients at the c.m. energy  $\sqrt{s_0} \approx 20 \text{ GeV}$  shows color-transparency for small dipole sizes,

$$\sigma_{LLCM}^{dp}(s_0, r_A) \approx 9.6 r_A^2 \quad (27)$$

and linear confining behavior at large dipole sizes,

$$\sigma_{LLCM}^{dp}(s_0, r_A) \propto |\vec{r}_A| . \quad (28)$$

Inserting eqs. (27) and (25) into (7), one obtains for the LO gluon distribution (7) at virtuality  $Q_0^2 = 1.8 \text{ GeV}^2$

$$xg^{(0)}(x, Q_0^2) = \frac{3}{4\pi^2 \alpha_s(Q_0^2)} \frac{1}{2C_A} 2 \cdot 9.6 = 0.81 . \quad (29)$$

With our result for  $\sigma_{LLCM}^{dp}(s_0, r_A)$ , the NLO gluon distribution (15) at the same virtuality reads

$$xg^{(1)}(x, Q_0^2) = 0.89 \ln \left( \frac{1}{x} \right) . \quad (30)$$

#### IV. DGLAP EVOLUTION AT HIGH $Q^2$

In this section we give the gluon and quark distributions at an initial scale  $Q_0^2$ . Their evolution to higher values of  $Q^2$  is obtained by the DGLAP equation

$$\begin{aligned} Q^2 \partial_{Q^2} \begin{pmatrix} q_i(x, Q^2) \\ \bar{q}_i(x, Q^2) \\ g(x, Q^2) \end{pmatrix} \\ = \frac{\alpha_s}{2\pi} \int_x^1 \frac{d\xi}{\xi} \begin{pmatrix} P_{q_i q_j} & 0 & P_{q_i g} \\ 0 & P_{q_i q_j} & P_{q_i g} \\ P_{gq} & P_{gq} & P_{gg} \end{pmatrix} \bigg|_{\frac{x}{\xi}} \begin{pmatrix} q_j(\xi, Q^2) \\ \bar{q}_j(\xi, Q^2) \\ g(\xi, Q^2) \end{pmatrix} , \end{aligned} \quad (31)$$

with the splitting functions  $P_{xy}$  being at leading order  $Q^2$  independent. We use the resulting gluon and quark distributions to compute the charm and proton structure function at different  $x$  and  $Q^2$  values.

The gluon distribution computed in the previous section reads

$$xg(x, Q_0^2) = A [1 + B \ln(1/x)] , \quad (32)$$

with  $A = 0.81$  and  $B = 1.1$  for  $Q_0^2 = 1.8 \text{ GeV}^2$ . Our result, however, is only expected to be valid at low  $x$  values. For large  $x$  values,  $x > x_{\text{GRV}} = 0.15$ , we use the Gluck-Reya-Vogt (GRV) gluon distribution [22]. To match to this gluon distribution at  $x = x_{\text{GRV}}$ , we introduce a scale  $x_0$  in our gluon distribution

$$G(x, Q_0^2) = xg(x, Q_0^2) = A [1 + B \ln(x_0/x)] \quad (33)$$

which takes into account the neglected constant term in the NLO calculation where only the leading  $\ln(1/x)$  terms have been kept. For  $Q_0^2 = 1.8 \text{ GeV}^2$  and  $x_{\text{GRV}} = 0.15$ , we obtain  $x_0 = 0.1454$ .

To calculate the proton structure function  $F_2^p(x, Q^2)$ ,

$$F_2^p(x) = x \sum_{\text{flavours}} e_q^2 [q(x) + \bar{q}(x)] ,$$

with the DGLAP evolution (31), we need quark and gluon distributions, since they are coupled to each other. For the computation of  $F_2^p(x, Q^2)$ , however, only two linear combinations of quark distributions are required

$$\begin{aligned} T &= x(u^+ + c^+ + t^+) - x(d^+ + s^+ + b^+) , \\ \Sigma &= x(u^+ + c^+ + t^+) + x(d^+ + s^+ + b^+) , \end{aligned}$$

since

$$F_2^p = \frac{5\Sigma + 3T}{18} ,$$

with  $q^+ = q + \bar{q}$  and  $q = u, d, s, c, t, b$ . Performing linear combinations in (31), we can directly check that  $T$ ,  $\Sigma$  and  $G$  evolve according to the following DGLAP equations

$$\begin{aligned} Q^2 \partial_{Q^2} T(x, Q^2) &= \frac{\alpha_s}{2\pi} \int_x^1 \frac{xd\xi}{\xi^2} P_{qq} \left( \frac{x}{\xi} \right) T(\xi, Q^2) , \\ Q^2 \partial_{Q^2} \begin{pmatrix} \Sigma(x, Q^2) \\ G(x, Q^2) \end{pmatrix} \\ &= \frac{\alpha_s}{2\pi} \int_x^1 \frac{xd\xi}{\xi^2} \begin{pmatrix} P_{qq} & 2n_f P_{qg} \\ P_{gq} & P_{gg} \end{pmatrix} \bigg|_{\frac{x}{\xi}} \begin{pmatrix} \Sigma(\xi, Q^2) \\ G(\xi, Q^2) \end{pmatrix} , \end{aligned}$$

which means that  $T$  evolves alone, while  $\Sigma$  is coupled with  $G$ .

We determine the  $x$ -dependence of the  $T$  and  $\Sigma$  distribution at the scale  $Q_0^2$  following the ideas from [23]. First, the  $T$ ,  $\Sigma$  and  $G$  distributions are required to have a common singularity structure in the complex  $j$ -plane according to Regge theory. Since the initial gluon distribution (33) has a double pole in  $j = 1$ , consequently, also the  $T$  and  $\Sigma$  distribution are required to have a double-pole pomeron term. Secondly, we add a reggeon contribution (coming from the exchange of meson trajectories  $a_0$  and  $f$ ) to the quark distribution. In the gluon distribution we neglect this term since the reggeon is expected to be constituted of quarks. Moreover, we expect that the pomeron, having vacuum quantum numbers, does not distinguish between quark flavours, i. e., the pomeron decouples from the  $T$  distribution. In contrast, the  $\Sigma$  distribution contains a pomeron and a reggeon component. The initial distributions, thus, read

$$\begin{aligned} T(x, Q_0^2) &= \tau x^{\alpha_0} (1-x)^\sigma, \\ \Sigma(x, Q_0^2) &= [a \ln(1/x) + b + dx^{\alpha_0}] (1-x)^\kappa \end{aligned} \quad (34)$$

with the reggeon intercept  $\alpha_0 = 0.4$  and the powers  $\sigma = 3$  and  $\kappa = 2$  of  $(1-x)$  taking into account daughter trajectories in Regge theory. For  $x > x_{\text{GRV}}$ , we again rely on the GRV distributions since our  $T$  and  $\Sigma$  distributions are only valid at small  $x$ . The parameters  $\tau$  and  $b$  are fixed to ensure continuity between our distributions and GRV's ones at  $x = x_{\text{GRV}}$ . Finally, we are left with 2 parameters,  $a$  and  $d$ , which we determine by fitting the  $F_2^p(x, Q^2)$  experimental data.

## V. RESULTS

With the previous  $T$ ,  $\Sigma$  and  $G$  distributions at  $Q_0^2 = 1.8 \text{ GeV}^2$  as an initial condition in the DGLAP equation, we have fitted the  $F_2^p$  experimental data within the domain

$$\begin{aligned} Q^2 &\geq Q_0^2 = 1.8 \text{ GeV}^2, \\ x &\leq x_{\text{GRV}} = 0.15, \\ \cos(\theta_t) &= \frac{\sqrt{Q^2}}{2 x m_p} \geq \frac{49 \text{ GeV}^2}{2 m_p^2}. \end{aligned} \quad (35)$$

Here  $m_p$  denotes the proton mass,  $\theta_t$  is the scattering angle in the  $t$ -channel and  $\cos(\theta_t)$  has been extended to the whole complex plane. The last condition of  $\cos(\theta_t)$  taken from [24] ensures that Regge theory is applicable. We have used 922 experimental points coming from H1 [25–27], ZEUS [28, 29], BCDMS [30], E665 [31] and NMC [32] to adjust our parameters within the given region. We

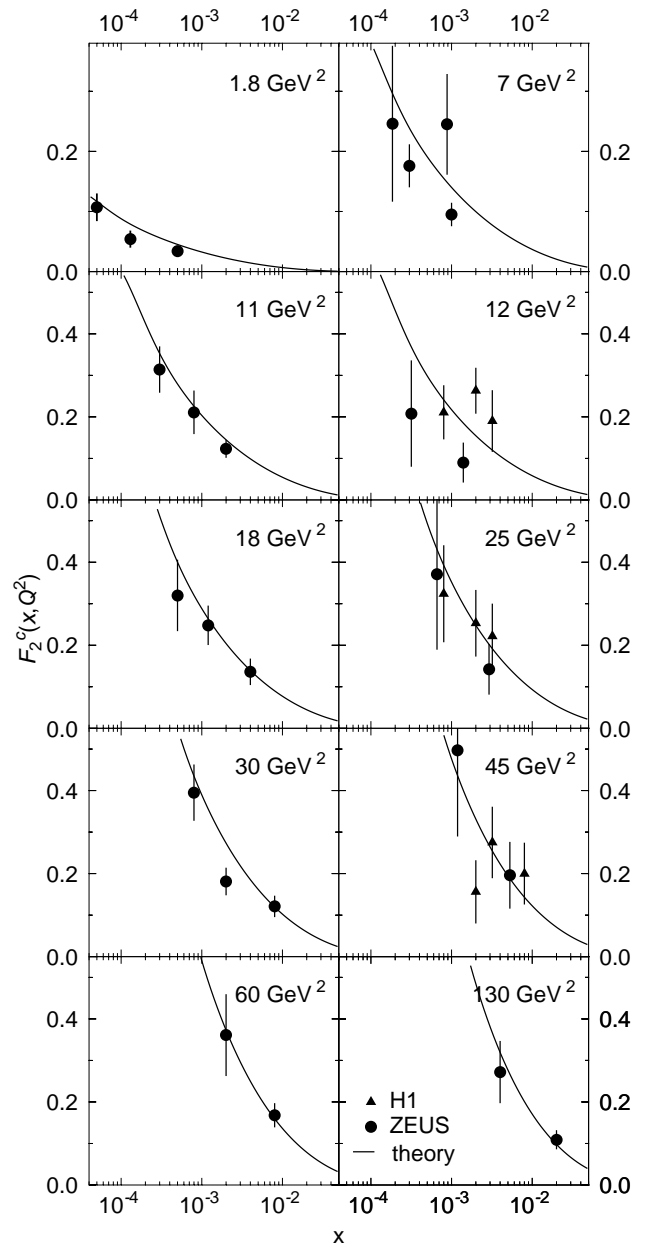


FIG. 7: The charm structure function,  $F_2^c(x, Q^2)$ , as a function of the Bjorken-variable  $x$  at different virtualities  $Q^2$ .

have obtained the following values

$$\begin{aligned} a &= 0.45933 \pm 0.00425, \\ b &= -1.9598 \quad (\text{fixed by continuity}), \\ d &= 6.0408 \pm 0.0456, \\ \tau &= 0.55628 \quad (\text{fixed by continuity}). \end{aligned}$$

In Figs. 8, 9 and 10 we show the results for the proton structure function,  $F_2^p(x, Q^2)$ , as a function of

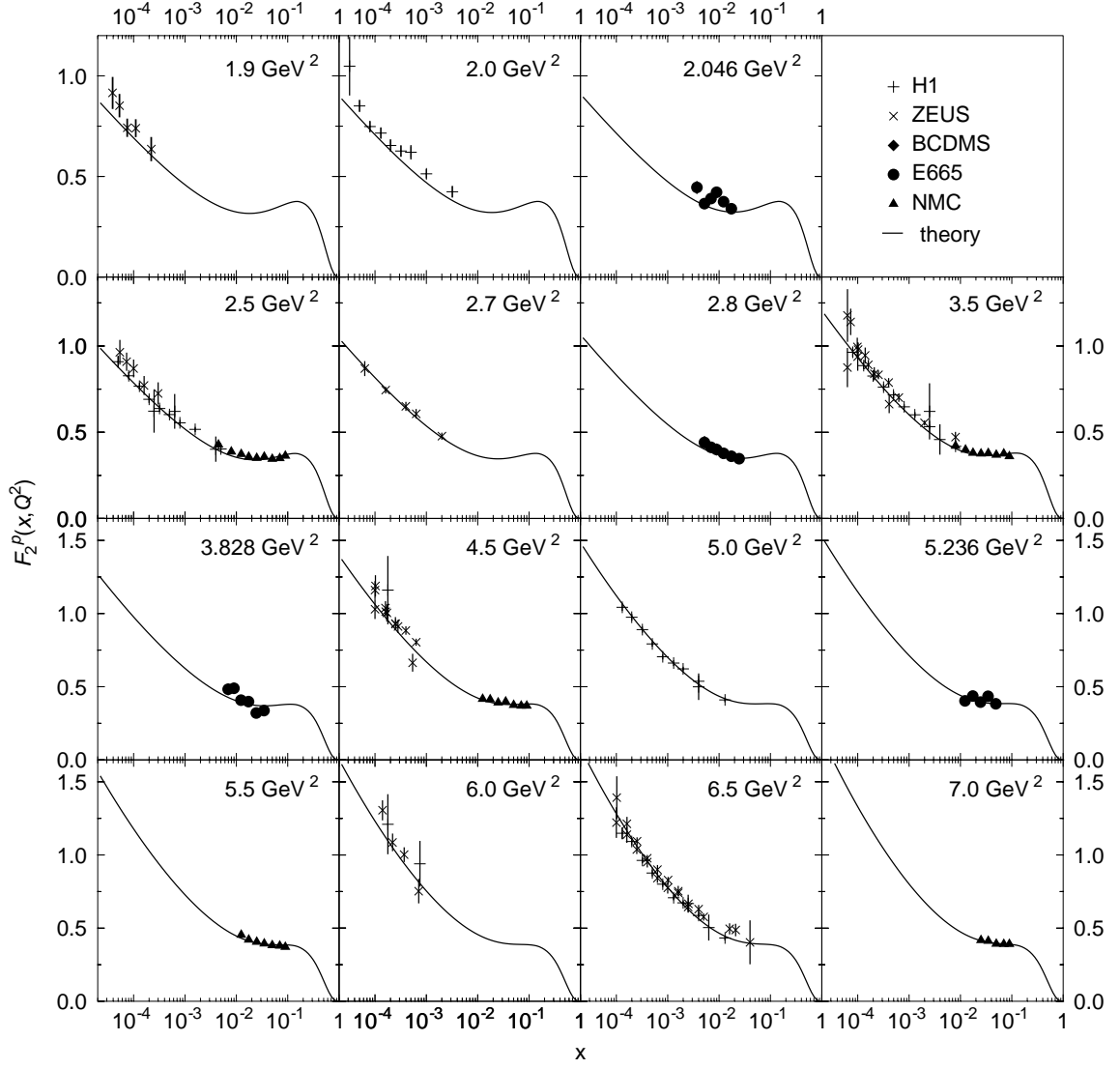


FIG. 8: The proton structure function,  $F_2^p(x, Q^2)$ , as a function of the Bjorken-variable  $x$  at low virtualities  $Q^2$ .

the Bjorken-variable  $x$  between the virtualities  $Q^2 = 1.8 \text{ GeV}^2$  and  $Q^2 = 3000 \text{ GeV}^2$ . Our results are in good agreement with experimental data for all  $x$  and  $Q^2$  values.

To test our gluon distribution, we compute the charm structure function which depends on the gluon distribution as follows [33]

$$F_2^c(x, Q^2) = 2e_c^2 \frac{\alpha_s(Q^2 + 4m_c^2)}{2\pi} \int_{ax}^1 d\xi g(\xi, Q^2 + 4m_c^2) f(x/\xi, Q^2),$$

with

$$\begin{aligned} f(x, Q^2) &= v \left[ (4 - \mu)x^2(1 - x) - \frac{x}{2} \right] \\ &\quad + L \left[ \frac{x}{2} - x^2(1 - x) + \mu x^2(1 - 3x) - \mu^2 z^3 \right], \\ \mu &= \frac{2m_c^2}{Q^2}, \\ v &= \sqrt{1 - \frac{2x\mu}{1-x}}, \\ L &= \log \left( \frac{1+v}{1-v} \right), \\ a &= 1 + 2\mu. \end{aligned}$$

We have adopted a value of 1.25 GeV for the charm quark mass. The predictions for  $F_2^c(x, Q^2)$  obtained from

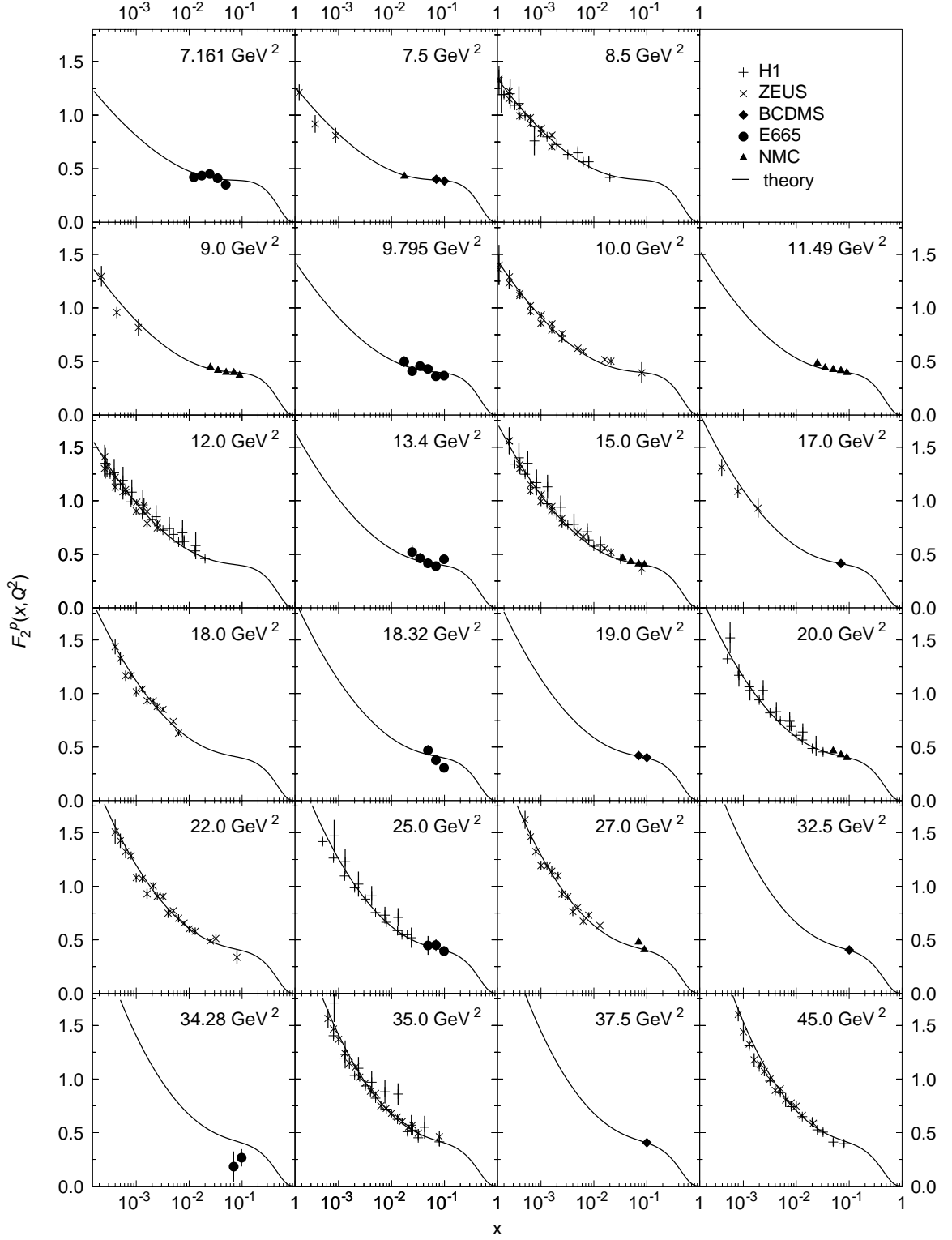


FIG. 9: The proton structure function,  $F_2^p(x, Q^2)$ , as a function of the Bjorken-variable  $x$  at middle-range virtualities  $Q^2$ .

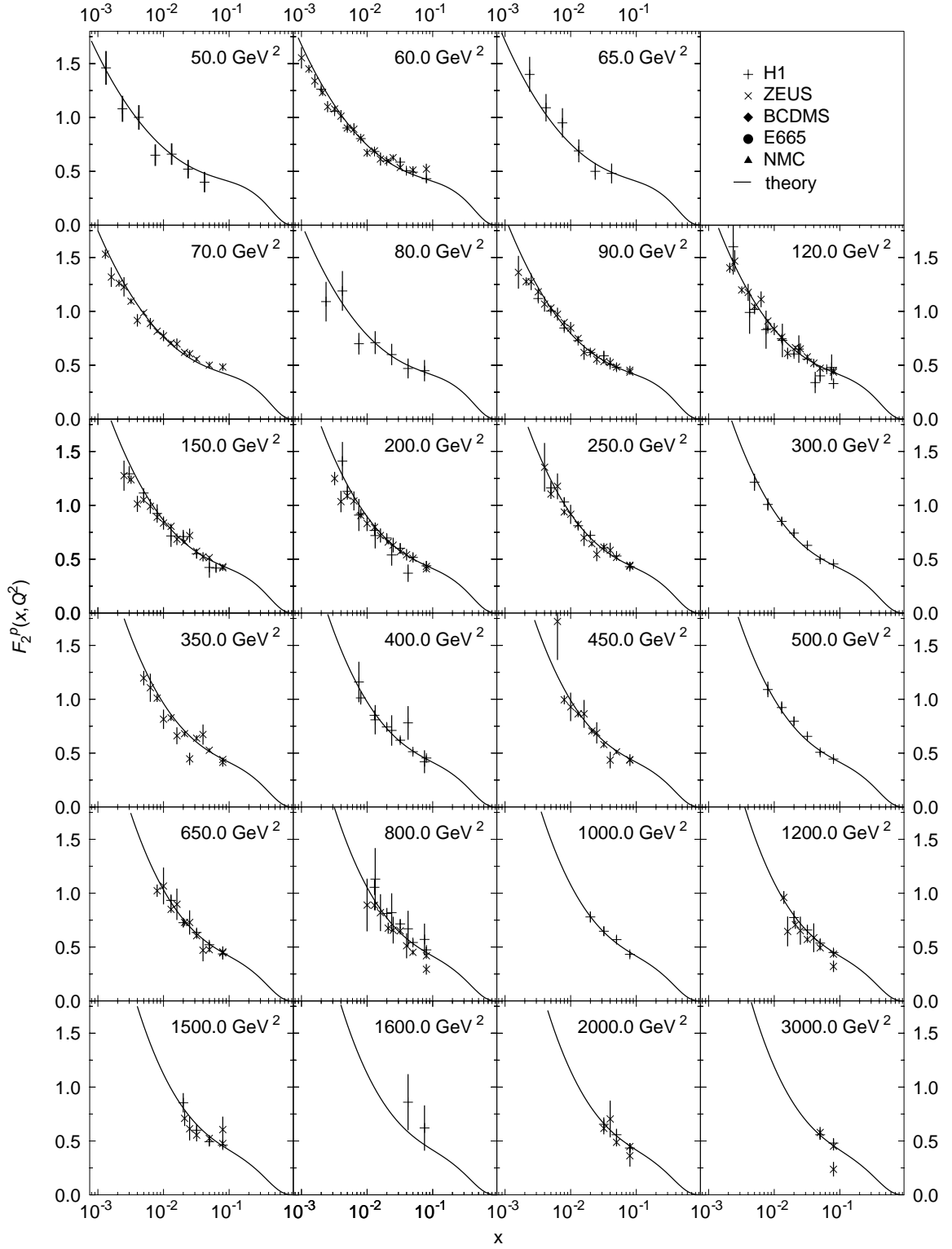


FIG. 10: The proton structure function,  $F_2^p(x, Q^2)$ , as a function of the Bjorken-variable  $x$  at high virtualities  $Q^2$ .



our model are presented together with the experimental HERA data [28, 34, 35] in Fig. 7. The good agreement of our predictions for  $F_2^c(x, Q^2)$  with experimental data clearly shows that we obtain a reasonable gluon distribution.

## VI. CONCLUSIONS

We have considered the interaction of a scalar “photon”, which directly couples to the gluons, with an external color field to extract the leading and next-to-leading order gluon distribution. We have closely followed the previous work by Dosch, Hebecker, Metz and Pirner [1], in which the semiclassical approach (where the partonic fluctuations of the “photon” interact with the proton in the eikonal approximation) has been compared with the parton model to get the gluon distribution of the proton. The leading order result is a constant while the next-to-leading order result has a  $\ln(1/x)$  rise at small  $x$ .

We have been able to relate the leading and next-to-leading order gluon distribution to the short and long distance behavior of the cross section of a dipole in the adjoint representation of  $SU(3)$  scattering off a proton, respectively. In addition, a gluon mass has been introduced to take into account nonperturbative effects in the

small- $k_\perp$  region of the perturbatively derived wave function of the two gluons emerging from the scalar “photon”, in analogy to the constituent quark mass in the quark-antiquark wave function. We have computed the adjoint dipole-proton cross section in the loop-loop correlation model [3] to obtain numerical results for the gluon distributions at the initial scale  $Q_0^2 = 1.8 \text{ GeV}^2$ .

Quark distributions at the same initial scale have been parametrized in line with Regge theory and the ideas leading to the gluon distribution. We have used DGLAP equations to evolve quark and gluon distributions to higher  $Q^2$  values. The charm and proton structure functions computed in the small- $x$  region are in good agreement with experimental HERA data over a large range of  $Q^2$  values.

## Acknowledgments

We would like to thank Arthur Hebecker and Stephane Munier for stimulating discussions. This research is partially funded by the INTAS project “Non-Perturbative QCD” and the European TMR Contract HPRN-CT-2000-00130. G. S. is supported by the National Fund for Scientific Research (FNRS), Belgium.

- 
- [1] H. G. Dosch, A. Hebecker, A. Metz and H. J. Pirner, Nucl. Phys. B **568** (2000) 287.
  - [2] A. H. Mueller, Nucl. Phys. B **335** (1990) 115.
  - [3] A. I. Shoshi, F. D. Steffen and H. J. Pirner, Nucl. Phys. A **709** (2002) 131.
  - [4] O. Nachtmann, Annals Phys. **209** (1991) 436.
  - [5] O. Nachtmann, in “Perturbative and Nonperturbative Aspects of Quantum Field Theory,” edited by H. Latal and W. Schweiger (Springer Verlag, Berlin, Heidelberg 1997) [hep-ph/9609365].
  - [6] A. Krämer and H. G. Dosch, Phys. Lett. B **252** (1990) 669.
  - [7] H. G. Dosch, E. Ferreira and A. Krämer, Phys. Rev. D **50** (1994) 1992.
  - [8] T. Regge, Nuovo Cim. **14**, 951 (1959);  
T. Regge, Nuovo Cim. **18**, 947 (1960);  
See for a modern overview of Regge theory and diffraction the books *Pomeron Physics and QCD* by S. Donnachie, G. Dosch, P. Landshoff and O. Nachtmann (Cambridge University Press, Cambridge, 2002), and *High-Energy Particle Diffraction* by V. Barone and E. Predazzi (Springer, Berlin, Heidelberg, 2002).
  - [9] V. N. Gribov and L. N. Lipatov, Yad. Fiz. **15** (1972) 781; L. N. Lipatov, Sov. J. Nucl. Phys. **20** (1975) 94; G. Altarelli and G. Parisi, Nucl. Phys. B **126** (1977) 298; Y. L. Dokshitz, Sov. Phys. JETP **46** (1977) 641.
  - [10] H. G. Dosch, T. Gousset and H. J. Pirner, Phys. Rev. D **57** (1998) 1666.
  - [11] M. Haas, “Berechnung der Gluonverteilung des Protons unter Benutzung zweier nichtperturbativer Modelle,” Diploma Thesis, Heidelberg 2000.
  - [12] W. Buchmüller, T. Gehrmann and A. Hebecker, Nucl. Phys. B **537** (1999) 477.
  - [13] A. I. Shoshi, F. D. Steffen, H. G. Dosch and H. J. Pirner, Phys. Rev. D **66** (2002) 094019.
  - [14] A. I. Shoshi, F. D. Steffen, H. G. Dosch and H. J. Pirner, “Confining QCD strings, Casimir scaling, and a Euclidean approach to high-energy scattering,” arXiv:hep-ph/0211287.
  - [15] A. I. Shoshi, “Anatomy of QCD strings and saturation effects in high-energy scattering,” arXiv:hep-ph/0302179.
  - [16] F. J. Wegner, J. Math. Phys. **12** (1971) 2259; K. G. Wilson, Phys. Rev. D **10** (1974) 2445.
  - [17] H. G. Dosch, T. Gousset, G. Kulzinger and H. J. Pirner, Phys. Rev. D **55** (1997) 2602.
  - [18] M. Wirbel, B. Stech and M. Bauer, Z. Phys. C **29** (1985) 637.
  - [19] L. Del Debbio, A. Di Giacomo and Y. A. Simonov, Phys. Lett. B **332** (1994) 111.
  - [20] M. Rueter and H. G. Dosch, Z. Phys. C **66** (1995) 245.
  - [21] A. I. Shoshi and F. D. Steffen, “Saturation effects in hadronic cross sections,” arXiv:hep-ph/0212070; A. I. Shoshi, F. D. Steffen and H. J. Pirner, “Gluon saturation and S-matrix unitarity,” arXiv:hep-ph/0205343.
  - [22] M. Gluck, E. Reya and A. Vogt, Eur. Phys. J. C **5**, 461 (1998).
  - [23] G. Soyez, Phys. Rev. D **67** (2003) 076001.
  - [24] J. R. Cudell, E. Martynov and G. Soyez, “t-channel unitarity and photon cross sections,” arXiv:hep-ph/0207196.
  - [25] C. Adloff *et al.* [H1 Collaboration], Eur. Phys. J. C **13**, 609 (2000).
  - [26] C. Adloff *et al.* [H1 Collaboration], Eur. Phys. J. C **19**,

- 269 (2001).
- [27] C. Adloff *et al.* [H1 Collaboration], Eur. Phys. J. C **21**, 33 (2001).
  - [28] J. Breitweg *et al.* [ZEUS Collaboration], Eur. Phys. J. C **12**, 35 (2000).
  - [29] S. Chekanov *et al.* [ZEUS Collaboration], Eur. Phys. J. C **21**, 443 (2001).
  - [30] A. C. Benvenuti *et al.* [BCDMS Collaboration], Phys. Lett. B **223**, 485 (1989).
  - [31] M. R. Adams *et al.* [E665 Collaboration], Phys. Rev. D **54**, 3006 (1996).
  - [32] NMC Collaboration: M. Arneodo *et al.*, *Nucl. Phys.* **B483** (1997) 3; *Nucl. Phys.* **B487** (1997) 3.
  - [33] R.G. Roberts, *The Structure of the Proton*, Cambridge University Press (1990).
  - [34] C. Adloff *et al.* [H1 Collaboration], Z. Phys. C **72**, 593 (1996).
  - [35] J. Breitweg *et al.* [ZEUS Collaboration], Phys. Lett. B **407**, 402 (1997).